A DOUBLE LOGISTIC MAP

LAURA GARDINI

Istituto di Scienze Economiche, Universita' di Urbino, 61029 Urbino (PS), Italy

RALPH ABRAHAM and RONALD J. RECORD

Department of Mathematics, University of California, Santa Cruz, CA 95064, USA

DANIELE FOURNIER-PRUNARET

Institut National des Sciences Appliquees, GESNLA, Avenue de Rangueil, 31077, Toulouse Cedex, France

Several endomorphisms of a plane have been constructed by coupling two logistic maps. Here we study the dynamics occurring in one of them, a twisted version due to J. Dorband, which (like the other models) is rich in global bifurcations. By use of critical curves, absorbing and invariant areas are determined, inside which global bifurcations of the attracting sets (fixed points, closed invariant curves, cycles or chaotic attractors) take place. The basins of attraction of the absorbing areas are determined together with their bifurcations.

1. Introduction

Sequences of bifurcations governing the route to chaos in one-dimensional endomorphisms have been extensively studied since 1975 [Mira, 1975; Gumowski & Mira, 1975a,b,c, 1980a,b], we refer to Mira [1987] for a review of the main results obtained so far. However, models reducing to two-dimensional endomorphisms are often obtained in several fields. Up to now, they have been mainly studied by numerical simulations. Several properties and bifurcations may be characterized, and basic tools of a theory obtained, by use of critical curves. Critical curves of a two-dimensional endomorphism, first considered by Gumowski and Mira, are generalizations of the critcal points of a one-dimensional endomorphism. In the latter case, the fundamental role played by critical points in determining and classifying global bifurcations (in particular homoclinic bifurcations) has been developed by several authors; besides the references cited above; see Collet & Eckmann [1980] and Devaney [1989]. The fundamental role played by critical curves in two-dimensional

endomorphisms has been developed by Mira since 1965 [Mira, 1965, 1966, 1969; Gumowski & Mira, 1977, 1978, 1980a,b] and recently by his collaborators (as we shall recall in Sec. 3).

In this paper we analyse an exemplary case. We make use of extensive simulations to show the particular role played by critical curves in determining properties and global bifurcations. The chosen example is the family of two-dimensional maps T_λ, which represents a coupled pair of logistic oscillators, $T_\lambda : \mathbb{R}^2 \to \mathbb{R}^2$, $(x, y) \to (x', y')$, as a function of a real parameter λ, defined by:

$$T \begin{cases} x' = (1 - \lambda)x + 4\lambda y(1 - y) \\ y' = (1 - \lambda)y + 4\lambda x(1 - x) \end{cases}, \quad \lambda \in [0, 1]. \quad (1)$$

To simplify the notation, in the following we shall write T instead of T_λ, as the dependence on the real parameter λ is understood. This map may be considered as a model of a two-dimensional oscillator. Several two-dimensional models of oscillators, derived from various applied fields (mainly physics and engineering, but also biology, ecology

and economics), have been published up to now. See, for example, Kaneko [1983], Hogg & Huberman [1984], Van Biskirk & Jeffries [1985], Lorenz [1989], Taylor [1990], De Sousa Vieira *et al.* [1991], Gaertner & Jungeilges [1992], Aicardi & Invernizzi [1992], and Lopez-Ruiz & Perez-Garcia [1992]. The map considered here is a particular case. However, the methodology we use may be applied to more general models.

The plan of the work is as follows. The fixed points of T, and their local stability analysis, will be determined in Sec. 2. In Sec. 3 we shall briefly recall some definitions and properties concerning the critical curves, to be used in subsequent sections. As it is immediate to see, T is a map with a nonunique inverse. The definition of its inverses (identifying their number, domains and codomains) is given in Sec. 4. In Sec. 5 we consider the regimes in which there exist two disjoint symmetric attractors, not fixed points of T, and in Sec. 6 the regimes in which T possesses a unique attractor, with symmetry. Inside the basins of attraction we shall determine the absorbing areas bounded by arcs of critical curves. The critical curves will be a basic analytical tool of our study. They will be used:

(a) to define the domains and codomains of the inverses of T (which in turn are the basis for interpretation of the dynamics of T);

(b) to determine absorbing areas, simply connected or annular;

(c) to characterize the global bifurcations (that is, qualitative changes in the dynamics of T, which are not related to the local bifurcations of some cycle, or periodic orbit, or T), and in particular contact bifurcations.

2. Symmetry and Fixed Points of T

In this section we establish symmetry properties in the dynamics of the double logistic map T and identify its fixed points. The eigenvalues (or characteristic multipliers) and eigenvectors of the derivative (or Jacobian matrix) of T, DT, evaluated at these points, are determined via classical analysis.

2.1. *Symmetry*

Let

$$\mathcal{P} : \mathbb{R}^2 \to \mathbb{R}^2, \quad (x, y) \to (y, x)$$

denote the reflection through the diagonal

$$\Delta = \{(x, x)\} \subset \mathbb{R}^2. \tag{2}$$

Proposition 2.1. *T is symmetric, or $T \circ \mathcal{P} = \mathcal{P} \circ T$.*

Proof. Let $f_\lambda(x, y) = (1 - \lambda)x + 4\lambda y(1 - y)$. Then

$$\begin{aligned}
\mathcal{P} \circ T(x, y) &= \mathcal{P}(T(x, y)) \\
&= \mathcal{P}(f_\lambda(x, y), \ f_\lambda(y, x)) \\
&= (f_\lambda(y, x), \ f_\lambda(x, y)) \\
&= T(y, x) = T \circ \mathcal{P}(x, y).
\end{aligned}$$

Thus T commutes with $\mathcal{P}$. We have the following corollaries:

Corollary 2.1. *The diagonal Δ is invariant:*

$$T(\Delta) = \Delta.$$

Corollary 2.2. *If P is a fixed point of T, so is $\mathcal{P}(P)$.*

Corollary 2.3. *If $P \in \Delta$ is a fixed point of T, then $r(1, 1)$, $r \in \mathbb{R}$, is an eigenvector of $DT(P)$.*

Corollary 2.4. *If $\{p_i, i \in \mathbb{N}\}$ is an orbit of T, so is $\{\mathcal{P}(p_i), i \in \mathbb{N}\}$.*

Corollary 2.3 will be proved in Sec. 2.4; the others are immediate. ∎

2.2. *Restriction of T to Δ*

We now focus on the dynamics of T restricted to the invariant diagonal Δ. Let $(z, z) \in \Delta$ and $(z', z') = T(z, z)$, then the restriction T_Δ reduces to a one-dimensional map, say

$$z' = g_\lambda(z), \tag{3}$$

where $g_\lambda(z)$ is a logistic function in nonstandard form:

$$g_\lambda(z) = (1 + 3\lambda)z - 4\lambda z^2. \tag{4}$$

For its graph, note that $g'_\lambda(z) = 1 + 3\lambda - 8\lambda z$ and $g''_\lambda(z) = -8\lambda < 0$ (for $\lambda > 0$). Thus, a local maximum (called a critical point of rank-0 of g_λ) exists for $\lambda > 0$, at $c_{-1} = 3/8 + 1/8\lambda$. The critical point of g_λ of rank-1 (in the sense of Julia and Fatou, that is,
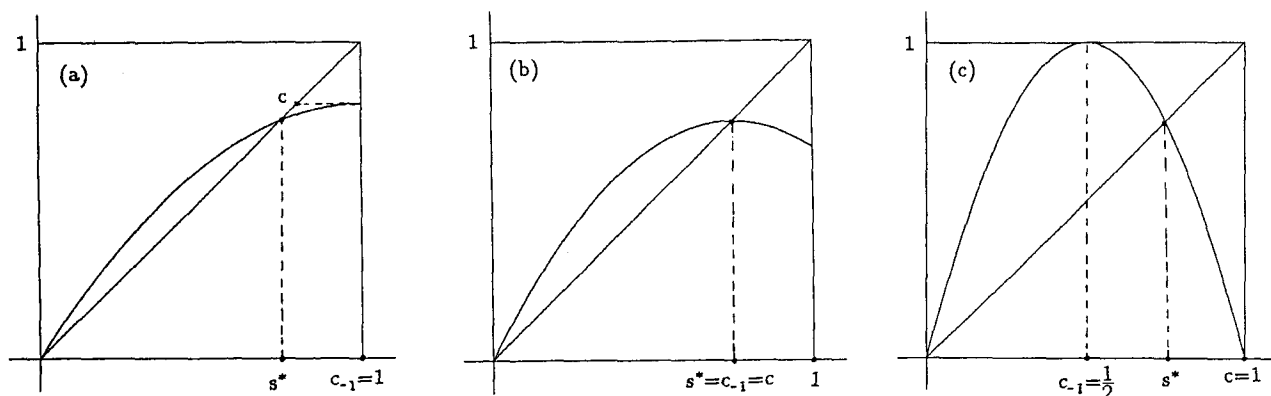
Fig. 1. Qualitative shapes of the function g_λ defined in (4). (a) $\lambda = 1/5$, $c_{-1} = 1$, $c = 4/5$; (b) $\lambda = 1/3$, $c_{-1} = c = 3/4$; (c) $\lambda = 1$, $c_{-1} = 1/2$, $c = 1$, $c_1 = 0$.

the locus of points having two coincident preimages of rank-1) is the point $c = g_\lambda(c_{-1})$, and the critical points of g_λ of rank-$(i+1)$ for $i \geq 1$ are the forward images (or iterates) $c_i = g_\lambda^{i+1}(c_{-1}) = g_\lambda^i(c)$. The fixed points of $g_\lambda(z)$, solutions of the equation $z = z(1+3\lambda-4\lambda z)$, are the origin, $z_1^* = 0$, and $s^* = 3/4$. About the multipliers, note that $g_\lambda'(0) = 1+3\lambda > 1$ and $g_\lambda'(3/4) = 1 - 3\lambda$, which decreases from 1 to -2 as λ increases from 0 to 1, going negative as λ passes $1/3$, and crossing the flip-bifurcation value -1 at $\lambda = 2/3$. The qualitative shapes of the function g_λ as λ increases from 0 to 1 are shown in Fig. 1 (for three particular positions).

The dynamics of the map g_λ can be obtained from that of the Myrberg's map, or of the standard logistic map, by an homeomorphism. A complete description of the complex bifurcation mechanism of type "box-within-a-box" (each box containing a sequence of flip-bifurcations known as Myrberg-cascade or Feigenbaum-cascade) can be found in Mira [1987]. We recall the bifurcation diagram, shown in Fig. 2, of z versus λ for $0.6 \leq \lambda \leq 1$ (the interval $0 < \lambda < 0.6$, in which the fixed point s^* is attracting, has been omitted). The value $\lambda = \lambda_{1s} \simeq 0.8566$ denotes the first accumulation value of the first Myrberg-cascade, related to the sequence of flip-bifurcations starting from that of the fixed point s^* (the flip-bifurcation of s^* opens the first box of the second kind, inside the first box of the first kind. See for example Mira [1987] for definitions). The value $\lambda = \lambda_{21}^* \simeq 0.8929$ is the closure of the first box of the second kind, homoclinic bifurcation of the fixed point s^* (that we shall reconsider in Sec. 5).

It is common nowadays to say that the dynamics of g_λ enters in a chaotic regime for $\lambda > \lambda_{1s}$,
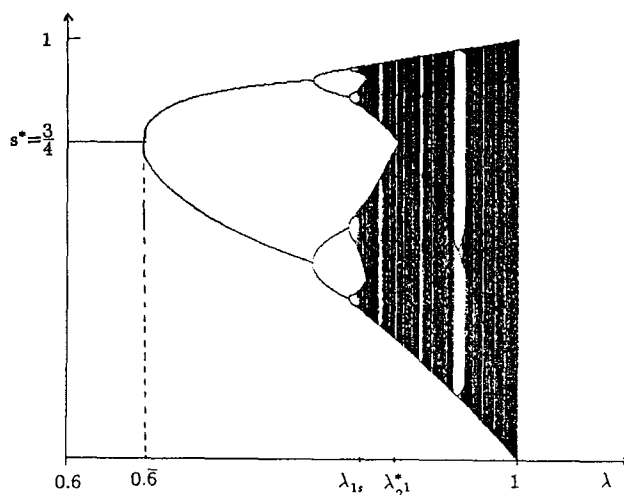
Fig. 2. Bifurcation diagram of g_λ defined in (4), z versus λ.

which is due to the fact that infinitely many repelling cycles exist, and these increase as λ increases up to $\lambda = 1$. We note however that for any given value of λ, beyond λ_{1s}, the asymptotic behavior of the generic trajectory in $(0,1)$ is either an attracting cycle or cyclic-invariant chaotic intervals. The attracting cycles are rarely observed (due to the existence of long chaotic transients coupled with numerical truncation errors), and we may speak, in these cases, of "*unstable-chaos*," reserving the term "*stable-chaos*" for those values of λ (bifurcation values) at which cyclic-invariant chaotic intervals exist. In short, we shall use the term "*chaotic regime*" or "*chaotic dynamics*" to denote either the case of unstable-chaos or that of stable-chaos, noticing that, generally, numerical observations deal with the case of unstable-chaos, and justifying our choice because in this case also closed invariant Cantor sets

exist, on which the dynamics of the map are chaotic (in the strict sense).

Similar considerations may be done for the dynamic behavior of the two-dimensional map T, and the same terms are used henceforth with the meaning given above.

We note also that for any value $\lambda > 2/3$, the (unique) attracting set of the map g_λ belongs to absorbing intervals or invariant intervals (defined in Sec. 3) bounded by critical points.

2.3. *Fixed points of T*

Besides an attracting set of T at infinity (or at infinite distance from the origin), on the Equator of Poincaré T possesses four fixed points at finite distance, belonging to the closed unitary square of the nonnegative quadrant $\mathbb{R}_+^2$, $\mathbb{R}_+^2 = \{(x, y) \in \mathbb{R}^2 : x \geq 0, t \geq 0\}$, where, as we shall see, the interesting dynamics of T take place.

From Corollary 2.1 and the discussion of g_λ above it follows that the origin $O = (0, 0)$ and the point $S^* = (3/4, 3/4)$ are two fixed points of T on Δ. We determine now the fixed points (x^*, y^*) with $x^* \neq y^*$ from direct computation. From the definition of T in (1) (putting $x' = x$ and $y' = y$) we get the following system:

$$x = 4y(1 - y) = f(y),$$

$$y = 4x(1 - x) = f(x),$$

where $f(x) = 4x(1 - x)$. It follows that if (x^*, y^*) is a fixed point of T with $x^* \neq y^*$ then x^* and y^* are points of a 2-cycle of $f(x)$. As the logistic function $f(x)$ possesses only one 2-cycle (see Fig. 3), we get two more fixed points of T, and no others exist. The values of x^* and y^*, coordinates of the two fixed points, say $P_1^* = (x^*, y^*)$ and $P_2^* = (y^*, x^*)$, symmetric with respect to Δ, can be obtained from the solutions, other than $x = 0$ and $x = 3/4$, of the equation $x = f(f(x))$. For $x \neq 0$ it it equivalent to

$$15 - 80x + 128x^2 - 64x^3 = 0$$

and, factoring out the other solution $x = 3/4$ already found, we have

$$\left(x - \frac{3}{4}\right)(16x^2 - 20x + 5) = 0,$$

so that, assuming $x^* > y^*$, we get $x^* = (5 + \sqrt{5})/8$ and $y^* = (5 - \sqrt{5})/8$ (that is, $x^* \simeq 0.904508$, $y^* \simeq 0.345442$).
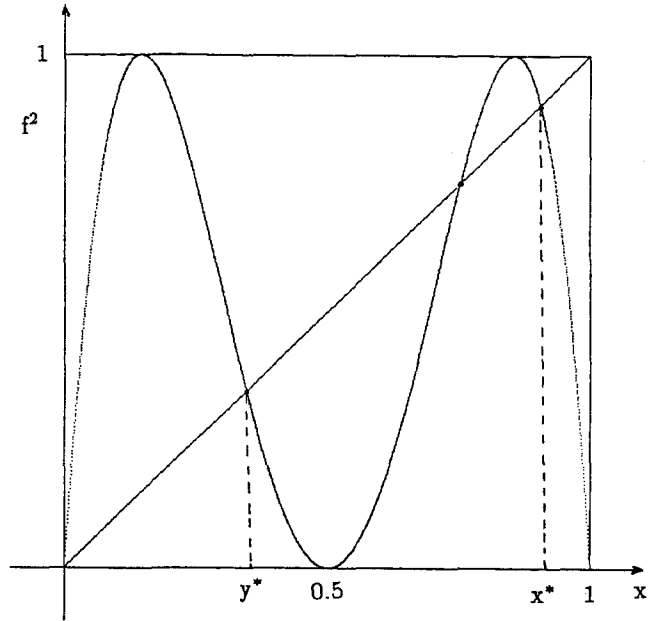

Fig. 3.   Graph of $f^2(x)$, $f(x) = 4x(1 - x)$.

In summary, the four fixed points of T are

$$O = (0, 0), \quad S^* = \left(\frac{3}{4}, \frac{3}{4}\right),$$

$$P_1^* = (x^*, y^*), \quad P_2^* = (y^*, x^*) \tag{5}$$

where

$$x^* = \frac{5 + \sqrt{5}}{8}, \quad y^* = \frac{5 - \sqrt{5}}{8}. \tag{6}$$

Note that, uncharacteristically, all the fixed points are independent of the control parameter λ.

2.4. *Eigenvalues and eigenvectors of DT at the fixed points*

The Jacobian matrix of T as a function of the state, $P = (x, y)$, and of the control parameter λ is

$$DT(x, y; \lambda) = \begin{bmatrix} 1 - \lambda & 4\lambda(1 - 2y) \\ 4\lambda(1 - 2x) & 1 - \lambda \end{bmatrix}. \tag{7}$$

We consider DT at the four fixed points, one at a time.

(1) At the fixed point $O = (0, 0)$ we have

$$DT(0; \lambda) = \begin{bmatrix} 1 - \lambda & 4\lambda \\ 4\lambda & 1 - \lambda \end{bmatrix},$$

with eigenvalues $s_1 = (1 + 3\lambda)$ [with eigenvector $r(1, 1)$] and $s_2 = (1 - 5\lambda)$ [with eigenvector $r(1, -1)$]. Thus the origin is repelling along Δ, as $s_1 > 1$ for
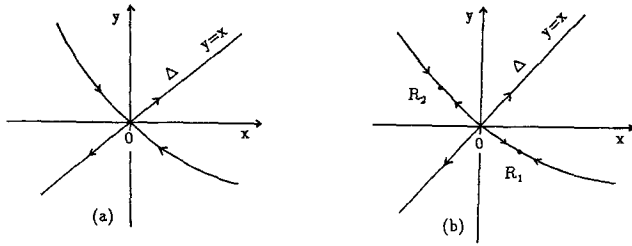
Fig. 4. Local invariant manifolds of the origin for (a) $\lambda < 0.4$; (b) $\lambda > 0.4$.

any $\lambda > 0$. Along the orthogonal direction we have attraction if $\lambda \in (0, 0.4)$ and repulsion, with $s_2 < -1$, if $\lambda > 0.4$. Thus, the origin is a saddle for $\lambda \in (0, 0.4)$, and a repelling node for $\lambda > 0.4$. The bifurcation occurring at $\lambda = 0.4$, a flip-bifurcation due to $s_2 = -1$ renders the attracting branch of the saddle repelling, on which a repelling 2-cycle saddle appears. See the schematic picture in Fig. 4, where the points of the 2-cycle, symmetric with respect to Δ, are named R_1 and R_2.

(2) At the fixed point $S^* = (3/4, 3/4)$ we have

$$DT(S^*; \lambda) = \begin{bmatrix} 1 - \lambda & -2\lambda \\ -2\lambda & 1 - \lambda \end{bmatrix}.$$

The eigenvalues of $DT(S^*)$ are $s_1 = (1 - 3\lambda)$ [with eigenvector $r(1, 1)$] and $s_2 = (1 + \lambda)$ [with eigenvector $r(1, -1)$]. Thus along a direction orthogonal to Δ the fixed point S^* is repelling for T, as $s_2 > 1$ for any $\lambda > 0$. Along the direction of Δ we have attraction if $\lambda \in (0, 0.\bar{6})$ and repulsion, with $s_1 < -1$, if $\lambda > 0.\bar{6}$. Stated otherwise, S^* is a saddle of T for $\lambda \in (0, 0.\bar{6})$ and a repelling node for $\lambda > 0.\bar{6}$. The bifurcation occurring at $\lambda = 0.\bar{6}$ (analogous to the one discussed above for the origin) creates a repelling two-cycle saddle on the line Δ, the points of which are denoted by Q_1 and Q_2. That is, at $\lambda = 0.\bar{6}$ the following transition occurs: S^* saddle of $T \to S^*$ repelling node of T+ two-cycle $Q_1 - Q_2$ saddle of T (and it corresponds to the flip-bifurcation of the fixed point s^* for the restriction of T to Δ, g_λ).

(3) At the fixed point $P_1^* = (x^*, y^*)$ we have

$$DT(P_1^*) = \begin{bmatrix} 1 - \lambda & 4\lambda(1 - 2y^*) \\ 4\lambda(1 - 2x^*) & 1 - \lambda \end{bmatrix},$$

where the values of x^* and y^* have been given in (6). After straightforward algebraic operations it may be seen that in this case we have a complex

pair of eigenvalues $s_{1,2} = (1 - \lambda) \pm 2\lambda i$, with modulus $|s_{1,2}| = 1 - 2\lambda + 5\lambda^2$, so that $|s_{1,2}| < 1$ for $\lambda \in (0, 0.4)$ and $|s_{1,2}| > 1$ for $\lambda > 0.4$. Thus, the fixed point P_1^* is an attracting focus for $\lambda \in (0, 0.4)$ and a repelling focus for $\lambda > 0.4$. A Neimark–Hopf bifurcation occurs at $\lambda = 0.4$.

(4) Due to the symmetry property of T, the local analysis of $DT(P_2^*)$ is the same as that of $DT(P_1^*)$, so that the fixed point P_2^* is an attracting focus for $\lambda \in (0, 0.4)$ and a repelling focus for $\lambda > 0.4$.

3. Critical Curves

In this section we recall some definitions and properties concerning the critical curves of a two-dimensional endomorphism, depending on a real parameter $\lambda : p' = T(p, \lambda) = (f(p, \lambda), g(p, \lambda))$, where $p = (x, y)$ is a point of $\mathbb{R}^2$, f and g are real-valued continuous functions, piecewise continuously differentiable. The point $p_i = T^i(p)$ for $i \geq 1$ is called the *image* (or consequent, or forward iterate) of *rank-i* of p. The *preimages* (or antecedents, or backward iterates) of *rank-i* of p are the points which are mapped into p after i applications of the map T. The *critical curve of rank-1* of T, denoted as LC, is the locus of points having at least two coincident preimages of rank-1. When f and g are continuously differentiable functions, LC is generally the image by T of LC_{-1}, where LC_{-1} is the locus of points in which the Jacobian of T vanishes:

$$LC_{-1} = \left\{ p \in \mathbb{R}^2 : |DT(p)| = 0 \right\};$$

$$LC = T(LC_{-1})$$

As LC_{-1} denotes the locus of the coincident preimages of LC, it results $LC = T(LC_{-1})$; note however that $LC_{-1} \subseteq T^{-1}(LC)$ and the inclusion is strict, $LC_{-1} \subset T^{-1}(LC)$ if T possesses more than two preimages (as in the case which interests us in this work). In such cases, the preimages of rank-1 of LC, distinct from LC_{-1}, are called *excess preimage curves*.

Critical curves of rank-$(i + 1)$ of T are the images of rank-i of the critical curve LC, that is, $LC_i = T^i(LC) = T^{i+1}(LC_{-1})$, $i \geq 0$, assuming $LC_0 = LC$. The critical curve LC separates the plane into open regions. The points of each region possess the same number of distinct preimages of rank-1.

Critical curves play the same important role as the critical points in one-dimensional endomorphisms in determining dynamic properties and

bifurcations in maps with a nonunique inverse. Several properties may be found in Gumowski & Mira [1980a], Barugola [1984, 1986], Cathala [1983, 1987, 1990], Barugola & Cathala [1992], Gardini [1991, 1992a,b], Gardini, Mira & Fournier [1992] and Gardini, Cathala & Mira [1992]. The critical curves have been used to determine the boundary of particular trapping or invariant regions, called absorbing areas and chaotic areas (inside which several bifurcations and transitions to chaotic regimes take place), and to characterize the bifurcations related to these sets. We recall below some definitions.

A subset A of the plane is called *trapping* if it is mapped into itself by T, $T(A) \subseteq A$; it is called *invariant* (or forward invariant) by T if $T(A) = A$, *backward invariant* by T if $T^{-1}(A) = A$.

An *absorbing area* d' is a closed subset of the plane, bounded by a finite number of arcs of critical curves, which is trapping, $T(d') \subseteq d'$, and for which a neighborhood exists, the points of which have an image of finite rank in the interior of d'. Its *basin of attraction* $\mathcal{D}(d')$ is an open set of points having an image of finite rank in d'. Its *frontier* (or *boundary*) $\mathcal{F} = \partial\mathcal{D} = \partial\bar{\mathcal{D}}$ is backward invariant for $T : T^{-1}(\mathcal{F}) = \mathcal{F}$. d' may contain one or several attractors, which may or may not be chaotic.

An *annular absorbing area* is an absorbing area of annular shape, that is, a simply connected area deprived of the points of a hole in its interior.

A *chaotic area* d is an invariant area of d', bounded by critical arcs or limit points of critical points, which contains a chaotic invariant set. In the simplest cases, the boundary of d is made up of a finite number of critical arcs. A chaotic area d may be destroyed or modified by a nonclassical bifurcation, called *contact bifurcation*, characterized by a contact between its boundary ∂d and the boundary $\mathcal{F}$ of its basin of attraction [Gumowski & Mira 1980a, pp. 368-371]. After the bifurcation, in the region which was occupied before by d, in short the "old area d," we may observe either a chaotic transient towards one attractor (at finite or infinite distance) or a fuzzy boundary (or fractal in the sense of Grebogi [Grebogi et al., 1983]) separating the basins of several attractors or chaotic areas. Several examples are described in Mira & Narayaninsamy [1992], and we shall see several of these different cases occurring in our map T.

Throughout this work, the arc of some curve connecting a point p to a point q will be denoted by the contracted form pq.

In general, an absorbing area d' can be determined with boundary $\partial d'$ made up of a finite number of critical arcs belonging to the images of an arc, say $b_0 a_0$ of LC_{-1}. Moreover, if a fixed point P^* belonging to d' is expanding, but is not a *snap-back repeller* (SBR henceforth), then an annular absorbing area $d'_a \subset d'$ can be obtained, with external and internal boundaries made up of a finite number of critical arcs belonging to the images of the arc $b_0 a_0$ of LC_{-1}. The bifurcation related to the appearance or disappearance of an annular chaotic area [or equivalently of a hole $W(P^*)$ surrounding the expanding fixed point] has been studied in Barugola et al. [1986] and Gardini [1992a].

We recall that a fixed point P^* of a map T is *expanding* if there exists a neighborhood U of P^* such that all the eigenvalues of the Jacobian matrix $DT(p)$ are greater than 1 in absolute value for all $p \in U$. A point q is *homoclinic* to P^* if there exists a positive integer j such that $T^j(q) = P^*$ and a sequence of preimages of q converges to P^*. P^* is an SBR if it is expanding and there exists a homoclinic point q of P^*.

The existence of infinitely many repelling cycles of T in a neighborhood of P^* when it is an SBR (i.e. the existence of chaos in the sense of Li & Yorke [1975]), has been proven by Marotto [1978] for endomorphisms of $\mathbb{R}^n$, $n \geq 2$. In Barugola et al. [1986] and Gardini [1992a] the bifurcation value is characterized in terms of critical curves as follows. The bifurcation, say at λ_r, which determines the transition of P^* to SBR is a homoclinic bifurcation which involves critical points of T, and:

(i) P^* is not an SBR iff all the rank-1 preimages of P^*, distinct from itself, are external to d';

(ii) an annular absorbing area $d'_a \subset d'$ exists iff P^* is not an SBR;

(iii) a value λ_r is the SBR bifurcation value iff (1) for $\lambda < \lambda_r$ all the rank-1 preimages of P^*, distinct from itself, are external to d'; and (2) at $\lambda = \lambda_r$ a preimage of rank-1 of P^* belongs to $\partial d'$, and it possesses a sequence of preimages entering U, U being a neighborhood of P^* such that all the eigenvalues of $DT(p)$ are greater than 1 in absolute value for any $p \in U$.

Note that the property stated above, that at $\lambda = \lambda_r$ a preimage of rank-1 of P^* belongs to $\partial d'$, coupled with the fact that $\partial d'$ consists of critical arcs, implies that at the SBR bifurcation value, all the critical arcs $T^k(b_0 a_0)$ for k greater than a suitable value pass through the fixed point P^*.

4. Critical Curves of T and Construction of the Frontier $\mathcal{F} = \partial \mathcal{D}$

The map T defined in (1) is clearly a map with a nonunique inverse. The critical curve LC of T (the locus of points having at least two coincident preimages of rank-1) is the image of the locus of points in which the Jacobian $|DT(p)|$ [the determinant of $DT(p)$ given in (7)] vanishes, that is,

$LC = T(LC_{-1})$ where LC_{-1} is the curve

$$LC_{-1} : \left(x - \frac{1}{2}\right)\left(y - \frac{1}{2}\right) = \frac{(1-\lambda)^2}{64\lambda^2}. \qquad (8)$$

LC_{-1} is an equilateral hyperbola of two branches. Let $LC_{-1} = LC_{-1,a} \cup LC_{-1,b}$, where $LC_{-1,a}$ denotes the upper branch (for $x > 1/2$ and $y > 1/2$) and $LC_{-1,b}$ denotes the lower branch [see Fig. 5(a)]. It follows also that the critical curve of rank-1, LC,

(a)

(b)

(c)
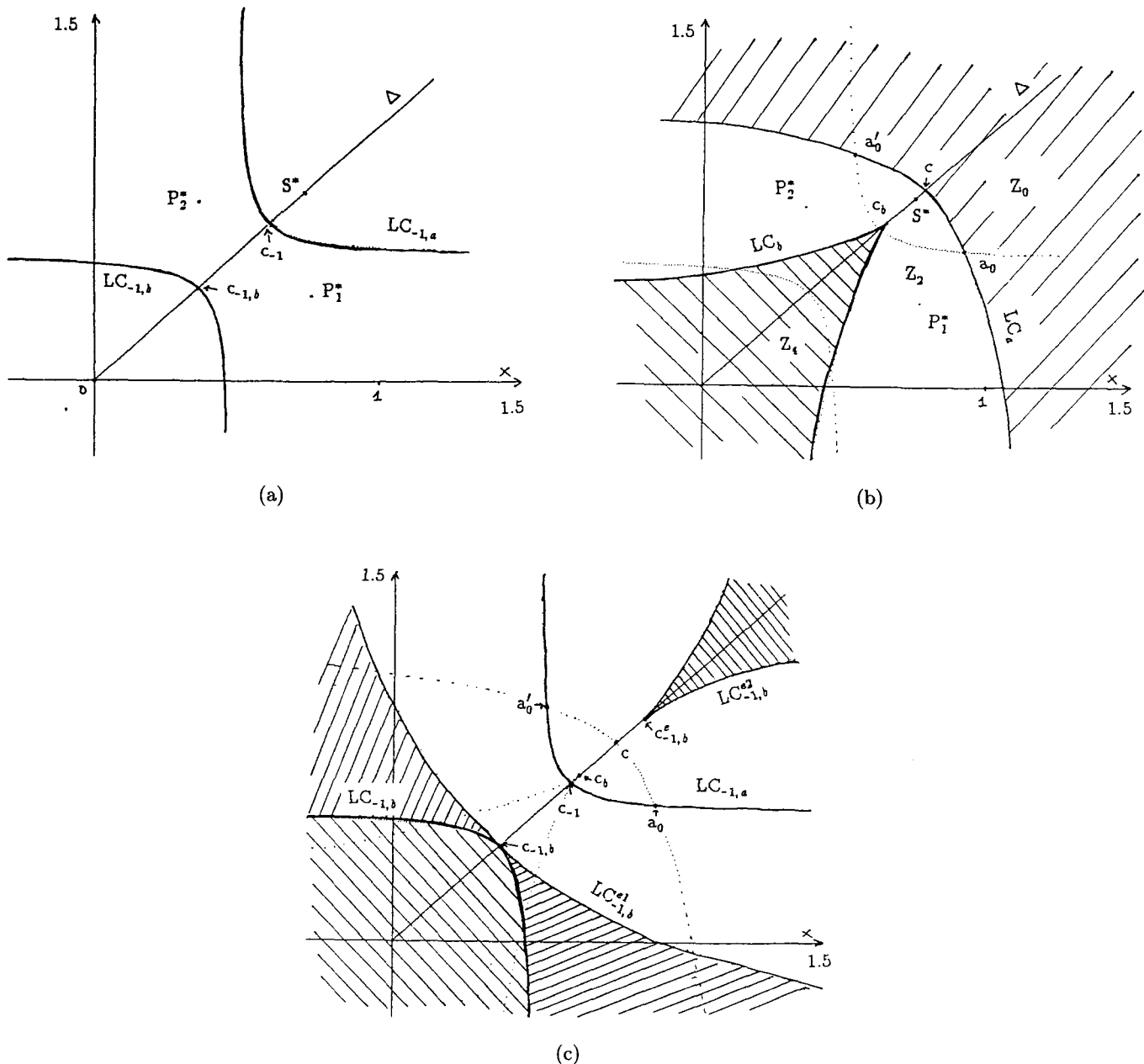
Fig. 5. $\lambda = 0.5$. (a) Curve $LC_{-1} = LC_{-1,a} \cup LC_{-1,b}$; (b) curve $LC = LC_a \cup LC_b$; (c) excess preimage curves $LC^{e1}_{-1,b}$ and $LC^{e2}_{-1,b}$.

consists of two branches, say $LC = LC_a \cup LC_b$, where $LC_a = T(LC_{-1,a})$ and $LC_b = T(LC_{-1,b})$. The two branches of LC_{-1} and those of LC are symmetric with respect to Δ. The qualitative shape of LC is shown in Fig. 5(b). LC separates the plane into three open regions, named Z_0, Z_2 and Z_4, locus of points having 0, 2 and 4 distinct preimages of rank-1 respectively [see Fig. 5(b)]. We note that a point of LC_a possesses only one preimage (that is, two coincident preimages) of rank-1 at a point of $LC_{-1,a}$, while a point p belonging to LC_b possesses two coincident preimages at a point of $LC_{-1,b}$ plus two distinct preimages of rank-1, called excess preimages of p (belonging to the excess preimages curves of LC_b). Numerically computed excess preimage curves of LC_b, denoted as $LC^{e1}_{-1,b}$ and $LC^{e2}_{-1,b}$, are shown in Fig. 5(c). These curves, together with the branches $LC_{-1,a}$ and $LC_{-1,b}$, separate the plane into disjoint regions which are distinct preimages of the regions Z_2 and Z_4. That is, a point $p \in Z_4$ has four preimages of rank-1, each belonging to one of the hatched regions of Fig. 5(c) (bounded by $LC_{-1,b}$ and its excess preimage curves $LC^{e1}_{-1,b}$ and $LC^{e2}_{-1,b}$), while a point $p \in Z_2$ has two distinct preimages in the remaining regions, one above and one below the branch $LC_{-1,a}$.

The critical points of the restriction of T to Δ, g_λ, already denoted by c, c_i, $i \geq 1$, in Sec. 2.2, belong to the intersection of the critical curves LC_a and $LC_{i,a}$ with Δ. That is, $c_{-1} = LC_{-1,a} \cap \Delta$, $c = LC_a \cap \Delta$ and $c_i = T^i(c) \in T^i(LC_a) \cap \Delta$, $\forall i \geq 1$. We denote also $c_{-1,b} = LC_{-1,b} \cap \Delta$, $c_b = LC_b \cap \Delta$ and $c_{i,b} = T^i(c_b) \in T^i(LC_b) \cap \Delta$, $\forall i \geq 1$.

In Fig. 5(b), we see that $LC_{-1,a} \cap LC_a$ consists of two points, named a_0 (in the region below Δ) and its symmetric a_0' (above Δ). We shall see, in Secs. 5 and 6, that for $\lambda \in (0.4, 1)$ an absorbing area d' is determined, bounded by critical arcs belonging to $a_0 a_0'$ of LC_a and its images.

4.1. Basins of attraction of the attracting fixed points of T

The intersection between the curves LC_{-1} and LC does not occur for any value of λ in the range $0 < \lambda \leq 0.4$. However in this range the fixed points P_i^*, $i = 1, 2$, are attracting, and the determination of an absorbing area is less important. We are interested in the direct determination of the basins of attraction $\mathcal{D}(P_i^*)$, $i = 1, 2$, of the attracting fixed points. As in this range of λ-values the origin O and the point S^* are two saddles of T, we may ex-

pect that the boundary of $\mathcal{D}(P_i^*)$ involves the stable sets of the saddles, $W^s(O)$ and $W^s(S^*)$. Moreover, denoting $\mathcal{D} = \mathcal{D}(P_1^*) \cup \mathcal{D}(P_2^*)$, then $\bar{\mathcal{D}}$ (where the overbar denotes the closure) is the locus of points having bounded trajectories in the plane, so that its frontier $\mathcal{F} = \partial \bar{\mathcal{D}}$, which we shall call the external frontier, is also the boundary of the basin of attraction of points at infinity, that is, of the basin of the Equator of Poincaré, and we may expect that $\mathcal{F}$ contains only the stable set of the origin.

We have performed numerical computations of the basins $\mathcal{D}(P_i^*)$ and of $\bar{\mathcal{D}}$, which we shall discuss below, distinguishing the intervals $0 < \lambda < 0.2$ and $0.2 < \lambda \leq 0.4$ and showing that at $\lambda = 0.2$ the first bifurcation of the two basins $\mathcal{D}(P_i^*)$ occurs. The bifurcation value $\lambda = 0.2$ is the value of λ at which occurs the first contact between $LC_{-1,b}$ and LC_b, at the point O. In particular, for $0 < \lambda < 0.2$, the critical points $c_{-1,b}$ and c_b belong to the negative quadrant of the plane, at $\lambda = 0.2$, $c_{-1,b} = c_b = O$, while for $\lambda > 0.2$, $c_{-1,b}$ and c_b belong to $\mathbb{R}_+^2$, so that the region Z_4 enters $\mathbb{R}_+^2$.

4.2. Basins in the first regime, $0 < \lambda < 0.2$

For $0 < \lambda < 0.2$, the origin belongs to Z_2 so that only one preimage of rank-1 of the origin exists distinct from O, say $O_{-1,1}$, belonging to Δ. The stable set $W^s(O)$ consists of two arcs, connecting O and $O_{-1,1}$, symmetric with respect to Δ. The stable set $W^s(S^*)$ is the segment $OO_{-1,1}$ on Δ, which is backward invariant by T. It follows that the external frontier $\mathcal{F} = \overline{W^s(O)}$ is made up of two arcs and their endpoints, while $\partial \mathcal{D}(P_1^*)$ consists of the segment $\overline{OO_{-1,1}} = \overline{W^s(S^*)}$ on Δ and the arc of $W^s(O)$ connecting O and $O_{-1,1}$ below Δ. The basin $\mathcal{D}(P_2^*)$ is the symmetric image of $\mathcal{D}(P_1^*)$ with respect to Δ, and both are simply-connected. Two examples are shown in Fig. 6.

4.3. Basins in the second regime, $0.2 < \lambda \leq 0.4$

For $0.2 < \lambda \leq 0.4$, we have again $\mathcal{F} = \overline{W^s(O)}$ made up of two arcs, and $\mathcal{D}$ becomes smaller as λ increases, maintaining the same qualitative shape [see the examples in Figs. 7(a) and 7(c)]. Changes occur in the stable set of the saddle S^*. The segment connecting the origin to c_b now belongs to the region Z_4. Thus $W^s(S^*)$ [which determines the boundaries of $\mathcal{D}(P_i^*)$], made up of the segment $OO_{-1,1}$ on
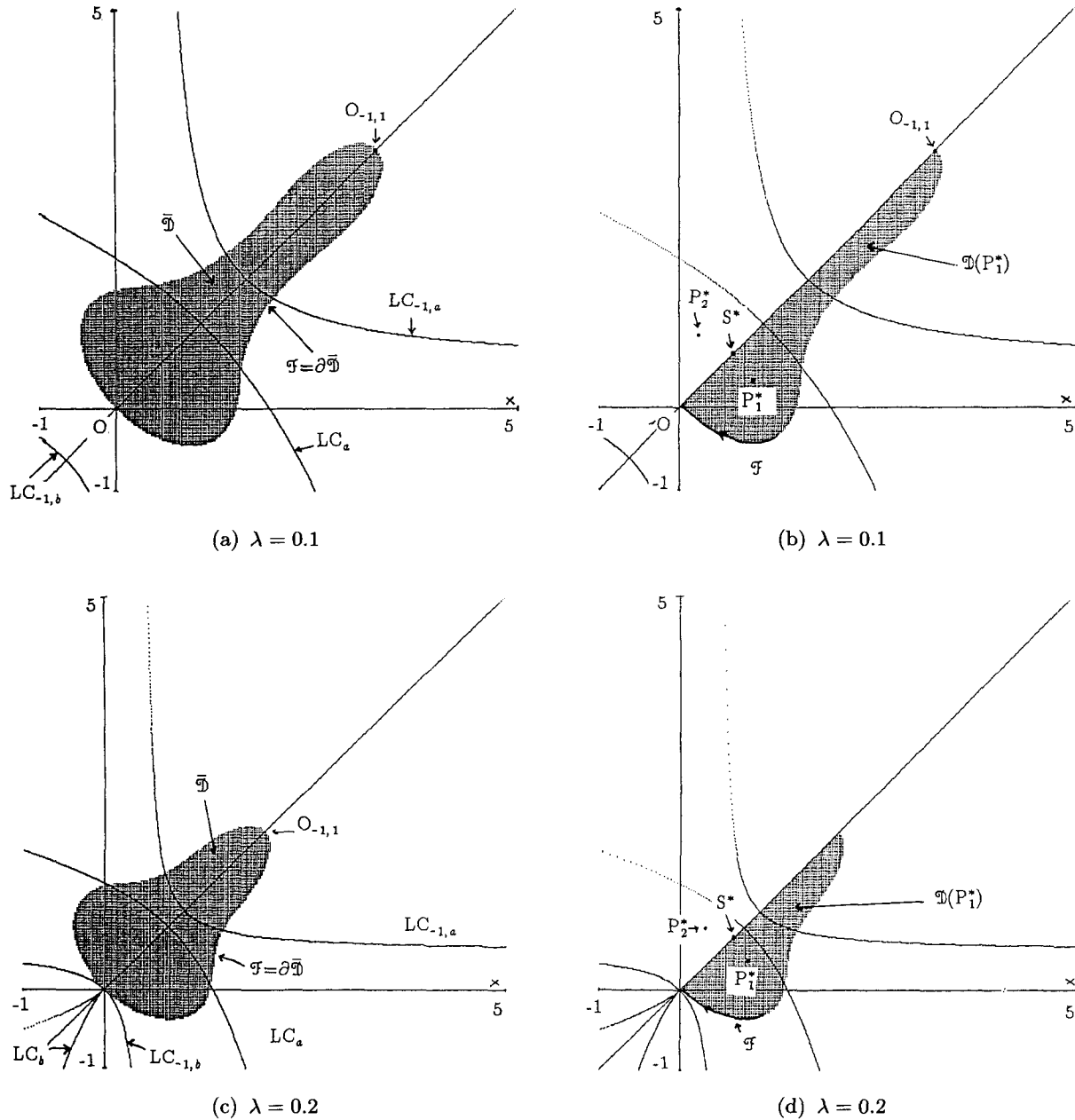
(a) $\lambda = 0.1$

(b) $\lambda = 0.1$

(c) $\lambda = 0.2$

(d) $\lambda = 0.2$

Fig. 6. (a) $\lambda = 0.1$, $\bar{\mathcal{D}}$ = shaded area, $\mathcal{F} = \partial\bar{\mathcal{D}}$; (b) $\lambda = 0.1$, $\mathcal{D}(P_1^*)$ = shaded area; (c) $\lambda = 0.2$, $\bar{\mathcal{D}}$ = shaded area, $\mathcal{F} = \partial\bar{\mathcal{D}}$; (d) $\lambda = 0.2$, $\mathcal{D}(P_1^*)$ = shaded area.

Δ and all its preimages of any rank, now has a more complex structure. It contains infinitely many arcs, which accumulate on the external frontier $\mathcal{F}$. Note that, in fact, the four preimages of the arc Oc_b are the arcs $Oc_{-1,b}$ and $c_{-1,b}^e O_{-1,1}$ on Δ, and $O_{-1,2}c_{-1,b}$ and $O_{-1,3}c_{-1,b}$ on the straight line issuing from $c_{-1,b}$ and orthogonal to Δ [see Figs. 7(b) and 7(d)]. The last two segments belong to Z_2 and possess two rank-1 preimages, one in Z_0 and one in Z_2, and so on. We have an infinite sequence of preimages of

two curve segments, one in Z_0 and one in Z_2 (issuing from points on Δ which accumulates on O and $O_{-1,1}$). It follows that the basin of attraction $\mathcal{D}(P_1^*)$ is no longer simply-connected. Let us call the *immediate basin*, $\mathcal{D}_0(P_1^*)$, the simply-connected component of $\mathcal{D}(P_1^*)$ containing the fixed point P_1^*. The total basin, $\mathcal{D}(P_1^*) = \cup_{n \geq 0} T^{-n}(\mathcal{D}_0(P_1^*))$, is disconnected and made up of infinitely many components, the preimages of any rank of the immediate basin. The boundary of each connected component of the
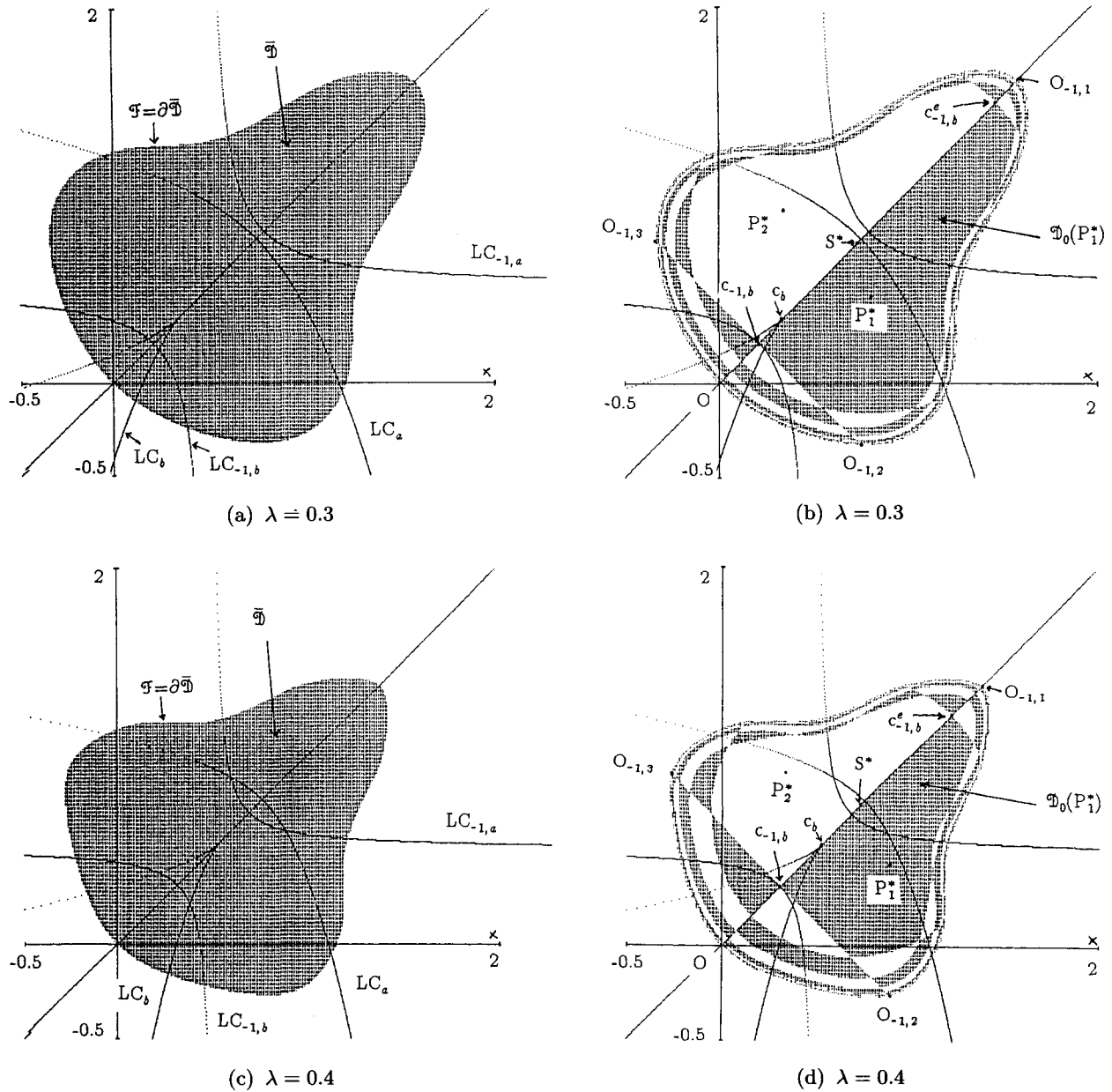
Fig. 7.   (a) $\lambda = 0.3$, $\bar{\mathcal{D}}$ = shaded area, $\mathcal{F} = \partial\bar{\mathcal{D}}$; (b) $\lambda = 0.3$, $\mathcal{D}(P_1^*)$ = shaded area; (c) $\lambda = 0.4$, $\bar{\mathcal{D}}$ = shaded area, $\mathcal{F} = \partial\bar{\mathcal{D}}$; (d) $\lambda = 0.4$, $\mathcal{D}(P_1^*)$ = shaded area.

total basin $\mathcal{D}(P_1^*)$ belongs to the stable set of S^* (because the boundary of the immediate basin belongs to the stable set of S^*). In the examples of Figs. 7(b) and 7(d) the shaded areas show the basin $\mathcal{D}(P_1^*)$, and the symmetric white areas comprise the basin $\mathcal{D}(P_2^*)$.

The total basins $\mathcal{D}(P_1^*)$ and $\mathcal{D}(P_2^*)$ will ultimately have a complicated structure of areas above and below the line Δ. There follows a sort of uncertainty with respect to the destiny of the points near the external frontier $\mathcal{F}$: we cannot predict if

a numerically computed trajectory will converge to P_1^* or P_2^*.

Note that the bifurcation of the basins occurring at $\lambda = 0.2$ is a global bifurcation characterized in terms of critical curves. In fact, it is due to the contact (and then intersection) of the critical curve LC_b with the backward invariant sets $\mathcal{F} = \overline{W^s(O)}$ and $\overline{W^s(S^*)}$, and the result of this contact is an explosion of the curve segments which constitute the stable set $W^s(S^*)$ (via the entrance of the region Z_4 bounded by LC_b in the area $\bar{\mathcal{D}}$).

Any point outside the area $\bar{\mathcal{D}}$ bounded by $\mathcal{F}$ has an unbounded trajectory, not only for the values of λ examined so far, but for any $\lambda > 0$.

4.4. Beyond the bifurcation at $\lambda = 0.4$

For $\lambda = 0.4$ the flip bifurcation of the origin and the Neimark–Hopf bifurcation of the fixed points P_i^*, $i = 1, 2$, simultaneously occur. The effect of these bifurcations is a new composition of the backward invariant set $\mathcal{F}$ and the appearance of new symmetric attracting sets. As already noticed, for $\lambda > 0.4$ an absorbing area d' can be computed, and $\mathcal{D}$ denotes its basin of attraction, whose boundary $\mathcal{F}$ separates in the plane those points having bounded trajectories from those with unbounded ones. This external frontier $\mathcal{F}$ is clearly related to the backward invariant set $\mathcal{F}$ previously described, in the sense that it is formed of arcs involving the origin and the periodic points bifurcated from it.

For $0.4 < \lambda < \lambda_b \simeq 0.7596$, the 2-cycle $R_1 - R_2$ bifurcated from O is a saddle so that $\mathcal{F} = \overline{W^s(R_1 - R_2)}$, and the stable set $W^s(R_1 - R_2)$ consists of arcs whose endpoints are the periodic points O, R_1, R_2 and their preimages of any rank [Mira, 1992]. The qualitative shape of $\mathcal{F}$ in this interval of λ-values is shown in the examples of Figs. 8(a) and 8(c).

As regards the study of the dynamics of T in $\mathcal{D}$, it may be divided into two regimes, called the third and fourth. In the third one, which shall be considered in Sec. 5, for $0.4 < \lambda < \lambda^*$ (where $\lambda^* \simeq 0.70209$ is a bifurcation value to be discussed below) $\mathcal{D}$ contains two disjoint symmetric attractors, belonging to two disjoint symmetric absorbing areas, d_1' and d_2' ($d_1' \cup d_2' \subset d'$), with two disjoint basins of attraction $\mathcal{D}_1$ and $\mathcal{D}_2$ respectively, such that $\mathcal{D} = \bar{\mathcal{D}}_1 \cup \bar{\mathcal{D}}_2$. In the fourth regime, considered in Sec. 6, for $\lambda^* < \lambda < 1$, $\mathcal{D}$ contains only one absorbing area d' (symmetric with respect to Δ). These regimes are separated by a contact bifurcation at $\lambda = \lambda^*$ between the boundaries of the invariant chaotic areas existing at $\lambda = \lambda^*$ and the boundaries of their basins of attraction, which will be discussed at the end of Sec. 5.

4.5. Basins in the third regime $0.4 < \lambda < \lambda^* \simeq 0.70209$

As stated above, for values of λ in the third regime, the map T possesses two disjoint symmetric attrac-

tors, say, $\mathcal{A}_1$ and $\mathcal{A}_2$. These are two closed invariant curves Γ_1 and Γ_2 (bifurcated from the focal fixed points P_1^* and P_2^*) while these are attracting, or cycles of T, or chaotic invariant sets, belonging to the absorbing areas d_1' and d_2'. It is clear that the two basins of attraction $\mathcal{D}_1$ and $\mathcal{D}_2$ are separated by the segment $OO_{-1,1}$ of the invariant line Δ and its preimages of any rank, that is, the set $\overline{W^s(S^*)}$ while the fixed point S^* is a saddle, i.e. for $\lambda \leq 0.\bar{6}$, and the closure of the stable set of the 2-cycle $Q_1 - Q_2$ on Δ, bifurcated from S^*, for $\lambda > 0.\bar{6}$ in this third regime. These boundaries are qualitatively similar to those already described above in the second regime. We note that with the preimages of rank 1, 2 and 3 of the segment $OO_{-1,1}$, the immediate basins, say $\mathcal{D}_{0,1}$ and $\mathcal{D}_{0,2}$, are obtained [two examples are shown in Figs. 8(b) and 8(d)]. That is, $\mathcal{D}_{0,1}$ is the largest simply connected area of $\mathcal{D}_1$ which includes $\mathcal{A}_1$, so that the total basin $\mathcal{D}_1$ itself is given by the union of all the preimages of $\mathcal{D}_{0,1}$, $\mathcal{D}_1 = \cup_{n \geq 0} T^{-n}(\mathcal{D}_{0,1})$. It is clear that infinitely many preimages of $\mathcal{D}_{0,1}$ exist, and the areas $T^{-n}(\mathcal{D}_{0,1})$ accumulate on the external frontier $\mathcal{F}$ as $n \to \infty$. The symmetric areas belong to $T^{-n}(\mathcal{D}_{0,2})$ and give $\mathcal{D}_2$.

As in the second regime, the total basins $\mathcal{D}_1$ and $\mathcal{D}_2$ will ultimately have a complicated structure of areas above and below the line Δ, and there is sensitive dependence on initial conditions near the external frontier $\mathcal{F}$: we cannot predict if a computed trajectory will fall eventually into $\mathcal{D}_{0,1}$ or $\mathcal{D}_{0,2}$.

In the example shown in Fig. 8(b), the attractor $\mathcal{A}_2$ in the immediate basin $\mathcal{D}_{0,2}$ is an invariant closed curve Γ_2, and its total basin is the collection of white areas. The black areas give the total basin $\mathcal{D}_1$. In Fig. 8(d) the attractor $\mathcal{A}_2$ in the immediate basin $\mathcal{D}_{0,2}$ (white area) is an invariant chaotic annular area; the value of λ is near the bifurcation value λ^*, as can be deduced from the closeness of the boundary of the invariant chaotic area to the boundary of its immediate basin.

4.6. Basins in the fourth regime $\lambda^* < \lambda < 1$

For $\lambda^* < \lambda < 1$ the complicated structure of two disjoint basins no longer exists, a unique absorbing area d' can be determined with the images of the arc $a_0 a_0'$ of LC_a. It includes the absorbing interval of the restriction of T to Δ, and its basin of attraction is the simply connected domain $\mathcal{D}$ bounded by the external frontier $\mathcal{F}$. The qualitative shape of $\mathcal{F}$ is

(a) $\lambda = 0.5$

(b) $\lambda = 0.5$

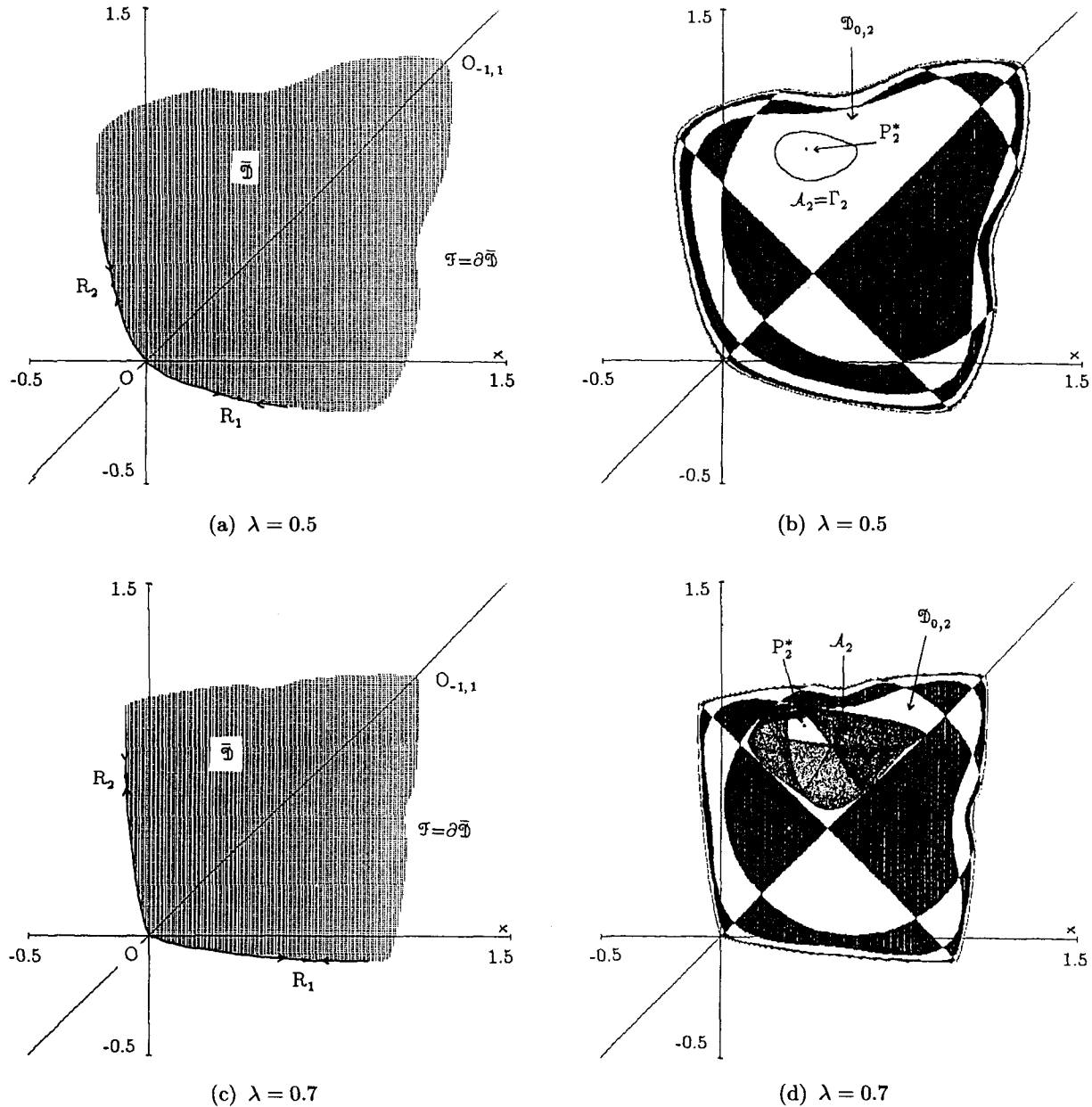(c) $\lambda = 0.7$

(d) $\lambda = 0.7$

Fig. 8.   (a) $\lambda = 0.5$, $\bar{\mathcal{D}}$ = shaded area, $\mathcal{F} = \partial\bar{\mathcal{D}}$; (b) $\lambda = 0.5$, $\mathcal{D}_1$ = black area; (c) $\lambda = 0.7$, $\bar{\mathcal{D}}$ = shaded area, $\mathcal{F} = \partial\bar{\mathcal{D}}$; (d) $\lambda = 0.7$, $\mathcal{D}_1$ = black area.

similar to that of Fig. 8(c) until the 2-cycle $R_1 - R_2$ is a saddle, i.e. for $\lambda^* < \lambda < \lambda_b \simeq 0.7596$. At $\lambda = \lambda_b$ a pitchfork bifurcation of this cycle occurs, such that for $\lambda > \lambda_b$ the 2-cycle $R_1 - R_2$ becomes a repelling node and a couple of 2-cycle saddles appear on $\mathcal{F}$. Thus, as λ increases, the dynamics of T in $\mathcal{D}$ becomes more complex, and the dynamics of T in the backward invariant set $\mathcal{F}$ also becomes more complicated. In fact, from the couple of 2-cycle saddles a sequence of bifurcations of type

box-within-a-box is initiated, so that the resulting set $\mathcal{F}$ becomes formed of invariant curve segments with a complex structure, and may also become a fractal set. These observations regarding the external frontier $\mathcal{F}$, which may be found in Mira [1992], need a deeper analysis; however we do not further pursue our study of $\mathcal{F}$ and in the following sections we will consider the dynamics of T inside $\mathcal{D}$.

We close this section observing that the last value of λ at which a bounded invariant set exists

is $\lambda = 1$, and at $\lambda = 1$, $\bar{\mathcal{D}}$ reduces to a closed unit square. This is a particular bifurcation value, discussed at the end of Sec. 6, as well as the "explosive" dynamics of T for the last regime, that is for $\lambda > 1$ (although not of interest in applications), when an absorbing region no longer exists and neither does $\mathcal{D}$.

5. Dynamics of T in the third regime

As we have described in Sec. 4, to study the dynamics of T in this regime ($0.4 < \lambda < \lambda^*$) it is sufficient to consider points of the immediate basin $\mathcal{D}_{0,1}$. In fact, symmetric dynamics occur in the symmetric immediate basin $\mathcal{D}_{0,2}$, and the destiny of the trajectory starting from any other point of the plane may be deduced from a figure like that of Figs. 8(b) or 8(d). That is, any point in the total basin $\mathcal{D}_1$ (respectively $\mathcal{D}_2$) has an image of finite rank in the immediate basin $\mathcal{D}_{0,1}$ (respectively $\mathcal{D}_{0,2}$). A point of the frontier of the total basins $\mathcal{D}_1$ or $\mathcal{D}_2$ not belonging to $\mathcal{F}$ has an image of finite rank in the portion of Δ which belongs to the frontier of $\mathcal{D}_{0,1}$ and $\mathcal{D}_{0,2}$, that is, converges to the attractor of the one-dimensional endormorphism $g_\lambda = T_\Delta$ which, in this regime, is either the fixed point S^*, for $\lambda \leq 0.\bar{6}$, or the attracting 2-cycle $Q_1 - Q_2$. Points outside $\bar{\mathcal{D}}$ have divergent trajectories.

For the reason explained above, the figures given in this section will show only an enlarged portion of $\mathcal{D}_{0,1}$ containing the attractor and the absorbing area of interest. Moreover, in order to avoid heavy notation, in the figures the curves $LC_{i,a}$ will be denoted henceforth as L_i for $i \geq -1$, and $L = LC_a$.

5.1. *Dynamics in* $\mathcal{D}_{0,1}$

The Neimark–Hopf bifurcation occurring at $\lambda = 0.4$ gives rise to an attracting closed invariant curve Γ_1 surrounding the repelling focus P_1^*. An absorbing area including Γ_1 may now be constructed by use of the procedures we describe below.

Consider the point a_0, intersection of $LC_{-1,a}$ and LC_a below Δ (that is, belonging to $\mathcal{D}_{0,1}$). By a_{-1} we denote its preimage of rank-1 belonging to $LC_{-1,a}$, while a_i, $i \geq 1$, denotes the image of rank-i of a_0 (a similar notation is used, that is, with integer indexes, to denote images of any point of the plane). For values of λ near the bifurcation value 0.4 the critical arcs $a_i a_{i+1} = T^i(a_{-1}a_0)$, $i \geq 0$, never intersect $LC_{-1,a}$ (and converge to the attracting set

Γ_1). Let $\bar{\lambda}$ be the value of λ at which an arc $a_i a_{i+1}$ becomes tangential to $LC_{-1,a}$, while for $\lambda > \bar{\lambda}$ an integer m exists such that $a_m a_{m+1}$ intersects $LC_{-1,a}$. Thus for $\lambda > \bar{\lambda}$, the images of the arc $a_{-1}a_0$ of $LC_{-1,a}$ intersect $LC_{-1,a}$ itself, and this permits us to apply a general procedure first described by Mira [1980] to determine the absorbing area. This is the reason why we discriminate between the two intervals of values for λ, and describe a different procedure in each of them. To determine the absorbing area d' we use Procedure 1 for $0.4 < \lambda \leq \bar{\lambda} \simeq 0.487$ and Procedure 2 for $\bar{\lambda} < \lambda \leq \lambda^* \simeq 0.70209$:

Procedure 1. Let h_{-1} be a point of $LC_{-1,a}$ such that $a_{-1}a_0 \subset a_{-1}h_{-1}$ and a critical arc $a_m h_m$ of $LC_{m,a}$ intersects $LC_{-1,a}$ at a point b_0, with $b_0 \in a_{-1}a_0$. Then the area d' bounded by the critical arcs

$$\partial d' = b_1 a_1 \cup a_1 a_2 \cup \cdots \cup a_m a_{m+1} \cup a_{m+1} b_1 \qquad (9)$$

is an absorbing area.

Procedure 2. Let m be the first integer such that the critical arc $a_m a_{m+1}$ of $LC_{m,a}$ intersects $LC_{-1,a}$, and let b_0 be the intersection point furthest from a_0. Then the area d' whose boundary is defined in (9) is an absorbing area.

An example in which d' is constructed by Procedure 1 is shown in Fig. 9. Procedure 1 gives an absorbing area d' which is contained in the region Z_2 below the curve $LC_{-1,a}$. This implies that of
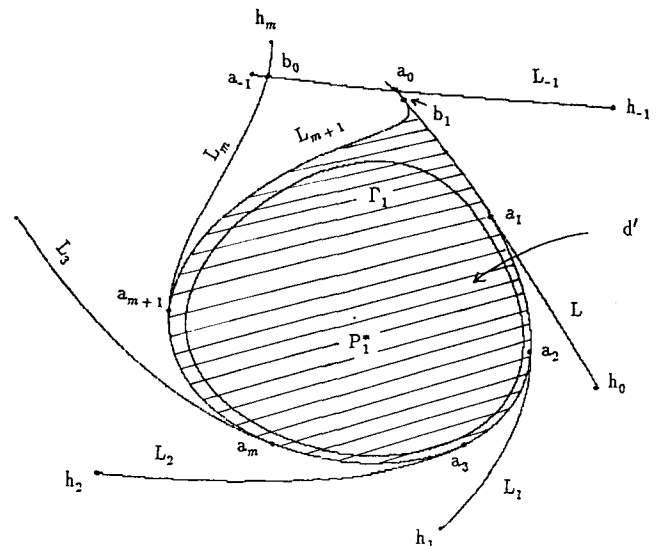

Fig. 9. $\lambda = 0.45$; absorbing area d' (hatched area), here $m = 4$.

the two distinct preimages of rank-1 of any point of d', only one belongs to d' itself; we call it the local inverse. The behavior of T in d' is like that of a map with a unique inverse, and with $T(d') \subset d'$, an invariant area cannot be obtained in a finite number of applications by T, as $T^{n+1}(d') \subset T^n(d')$ for any $n \geq 0$. Thus we have $\lim_{n \to \infty} T^n(d') = \cap_{n>0} T^n(d') = V$, where V is a closed invariant area bounded by a closed invariant curve. Here we have $\partial V = \Gamma_1$.

As in the interior of V the local inverse of T is contractive with P_1^* being an attracting focus, we may conclude that Γ_1 is globally attracting in $\mathcal{D}_{0,1}$, apart from the repelling focus P_1^*.

For $\lambda > \bar{\lambda}$ the images of the critical arc $a_0 a_1$ of LC_a intersect $LC_{-1,a}$ and we use Procedure 2 to determine an absorbing area. In the example shown in Fig. 10(b) the boundary of d' is formed by six critical arcs: $b_1 a_1 \subset LC_a$, $a_1 a_2 \subset LC_{1,a}$, $a_2 a_3 \subset LC_{2,a}$, $a_3 a_4 \subset LC_{3,a}$, $a_4 a_5 \subset LC_{4,a}$, $a_5 b_1 \subset LC_{5,a}$.

Qualitative changes occur in the absorbing area d', not only because we use Procedure 2 (as it is easy to see that it coincides with Procedure 1 assuming $h_{-1} = a_0$), but due to the fact that for $\lambda > \bar{\lambda}$, d' possesses a portion, say δ_0, above $LC_{-1,a}$. In fact, a first consequence is that now an annular absorbing area may be constructed (as discussed below), and a second consequence is that now in d' dynamics typical of a two-dimensional endomorphism may appear. In fact, the area $\delta_1 = T(\delta_0)$ is the locus of points of d' having two distinct preimages of rank-1 in d' itself, one in δ_0 and one below the curve $LC_{-1,a}$. For this reason the points of δ_1 are called "branching points," and we refer to δ_1 as "the area of branching points."

Let us first describe the two bifurcations of Γ_1 that can be characterized in this regime. The first one is due to the tangency, and then intersection, of Γ_1 with $LC_{-1,a}$. The contact between Γ_1 and $LC_{-1,a}$ occurs at $\lambda = \lambda_1$, $\lambda_1 \simeq 0.48735$. The shape of Γ_1 is smooth and similar to an oval for $0.4 < \lambda < \lambda_1$, but a qualitative change occurs in its shape as λ crosses the bifurcation value λ_1, because this contact causes the appearance of oscillations in Γ_1. At $\lambda = \lambda_1$ the invariant attracting curve Γ_1 is tangential to $LC_{-1,a}$, and thus to all the critical curves LC_i for any $i \geq 0$; while for $\lambda > \lambda_1$, Γ_1 intersects $LC_{-1,a}$ in two points and possesses a portion of curve above $LC_{-1,a}$. Thus, the qualitative change of Γ_1 (already described in Gumowski & Mira [1980b, p. 217]) is due to the portion of the invariant curve

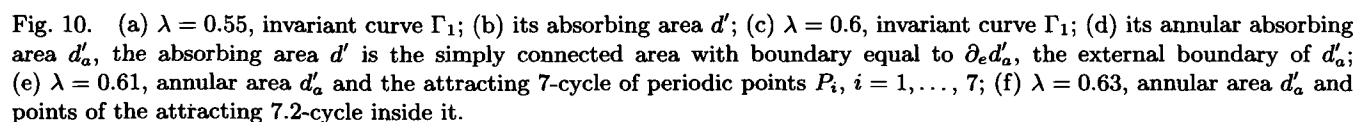above $LC_{-1,a}$ which is folded on LC_a and causes the deformation.

We note that any point of Γ_1 has two distinct preimages of rank-1, only one of which belongs to Γ_1. Thus, before the contact, when Γ_1 is below the curve $LC_{-1,a}$, its rank-1 distinct preimage, say $\Gamma_{1,-1}$, is above $LC_{-1,a}$ and disjoint from Γ_1. At the contact of Γ_1 with $LC_{-1,a}$ we also have a contact between the invariant curve and its rank-1 preimage; $\Gamma_1 \cap \Gamma_{1,-1} = \Gamma_1 \cap LC_{-1,a} = \Gamma_{1,-1} \cap LC_{-1,a}$ is the contact point at $\lambda = \lambda_1$, while for $\lambda > \lambda_1$ it is the set of intersection points between Γ_1 and the curve LC_{-1} [see the points p_0 and q_0 of $LC_{-1,a}$ in Fig. 10(a)].

The first bifurcation of Γ_1, at $\lambda = \lambda_1$, causes the appearance of smooth oscillations on the invariant curve. The oscillations become more pronounced (and the annular area becomes wider) after the second bifurcation of Γ_1, which occurs, in our example, when the invariant curve crosses $LC_{-1,a}$ in the two points a_{-1} and a_0, at $\lambda = \lambda_2 \simeq 0.505$. This is due to the fact that after this crossing, the invariant curve Γ_1 will be tangential to LC_a in two points, one above and one below $LC_{-1,a}$ [see the points p_1 and q_1 in Fig. 10(a), rank-1 images of the points p_0, external to $a_{-1} a_0$, and q_0, internal to $a_{-1} a_0$].

For $\lambda > \bar{\lambda}$, while P_1^* is not an SBR, not only can a simply-connected absorbing area d' be constructed, but also an annular absorbing area d'_a, $d'_a \subset d'$, giving a hole surrounding P_1^*, defined as $H(P_1^*) = d' \backslash d'_a$. We call the *internal boundary of* d'_a, $\partial_i d'_a$, the boundary of $H(P_1^*)$, while the *external boundary* of d'_a, $\partial_e d'_a$, is the residual part of the boundary of the annular area, so that $\partial d'_a = \partial_i d'_a \cup \partial_e d'_a$. The annular absorbing area can be constructed having the external boundary $\partial_e d'_a = \partial d'$ and the internal boundary made up of critical arcs belonging to $T^i(\gamma_0)$ for $i = 1, \ldots, K$ for a suitable $K \geq m$, where $\gamma_0 = a_{-1} a_0$ if b_0 is internal to the interval $a_{-1} a_0$, $\gamma_0 = b_0 a_0$ otherwise (in particular, for $\lambda \geq \lambda_2$ it is $\gamma_0 = b_0 a_0$).

In the example of Fig. 10(d) the boundary of d' is formed by critical arcs belonging to the images of rank-i, $i = 1, \ldots, 5$, of the arc $b_0 a_0$, while the internal boundary of d'_a is formed by critical arcs belonging to 7 images of $b_0 a_0$. In the examples of Figs. 10(e) and 10(f), the boundary of d'_a (both internal and external) is formed by arcs belonging to 6 images of $b_0 a_0$.

At first the annular absorbing area d'_a is very thin, almost indistinguishable from Γ_1, but it

Fig. 10.   (a) $\lambda = 0.55$, invariant curve Γ_1; (b) its absorbing area d'; (c) $\lambda = 0.6$, invariant curve Γ_1; (d) its annular absorbing area d'_a, the absorbing area d' is the simply connected area with boundary equal to $\partial_e d'_a$, the external boundary of d'_a; (e) $\lambda = 0.61$, annular area d'_a and the attracting 7-cycle of periodic points P_i, $i = 1, \ldots, 7$; (f) $\lambda = 0.63$, annular area d'_a and points of the attracting 7.2-cycle inside it.

becomes wider on increasing λ. Equivalently, the hole surrounding P_1^*, $H(P_1^*) = d' \backslash d'_a$, decreases.

We have not yet spoken about the points which are attracted into this annular area. From the construction of d' it follows that any point of the

immediate basin $\mathcal{D}_{0,1}$ has an image of finite rank inside d', and inside d' any point apart from P_1^* has an image of finite rank inside the annular area d'_a. To see this we observe that the points of the hole $H(P_1^*)$ possess two distinct preimages of rank-1, one

outside the hole and one inside the hole. That is, T is locally invertible in the hole $H(P_1^*)$, and this inverse possesses an attracting focus in P_1^*. Thus, the asymptotic behavior of T must be examined inside the annular area d_a'.

We conjecture that while an attracting curve Γ_1 exists, it is globally attracting in d_a'. We cannot prove that no cycle exists outside Γ_1 by direct computation; however we can motivate our conjecture as follows. The dynamical behavior of the images of the arc γ_0 is indicative of the generic trajectory in d_a', and we observe numerically that an image of high rank is almost indistinguishable from Γ_1. As the boundary of $T^n(d_a')$ consists of critical arcs belonging to the images of γ_0, for any $n \geq 0$, it follows that $\cap_{n>0} T^n(d_a') = \Gamma_1$ in our example.

As T_{Γ_1} has a unique inverse on Γ_1, T must have on Γ_1 the dynamics of an invertible map of the circle into itself (in the sense that T_{Γ_1} is homeomorphic to such a map). Thus, the trajectories on the attracting curve Γ_1 may be periodic (when the rotation number is rational) or quasiperiodic (when the rotation number is irrational). Cycles on Γ_1 appear and disappear via saddle-node bifurcations, and boxes-in-files bifurcations (described in Mira [1987]) have been observed.

A specific 7-cycle on Γ_1 is shown in Fig. 10(e). It is specific because it is related (in some way, as yet unknown) to the "disappearance" of the attracting curve Γ_1. The 7-cycle is born in a saddle-node bifurcation, and the invariant curve Γ_1 may still exist, made up of the invariant manifolds (heteroclinic connections) between the attracting and repelling points of the two 7-cycles (an attracting node and a saddle) born at this bifurcation. We note however that for the attracting 7-cycle node shown in Fig. 10(e) the eigenvalue associated with the direction transverse to the closed curve is negative (which is possible only in endomorphisms), and it will cross the value -1. That is, the stable 7-cycle undergoes a flip-bifurcation, it becomes a saddle and an attracting 7.2-cycle appears [see Fig. 10(f)]. This is the first of a sequence of bifurcations of type box-within-a-box (that is, no longer boxes-in-files), and this marks the difference between this 7-cycle and the cycles of T occurring before on Γ_1. The cascade of flip and fold bifurcations (similar to those occurring in a one-dimensional endomorphism), gives rise to attracting sets which no longer belong to a curve of the plane. An example is shown in the 7.2-band chaotic attractor of Fig. 11(a), which has a fractal dimension (between 1 and 2).
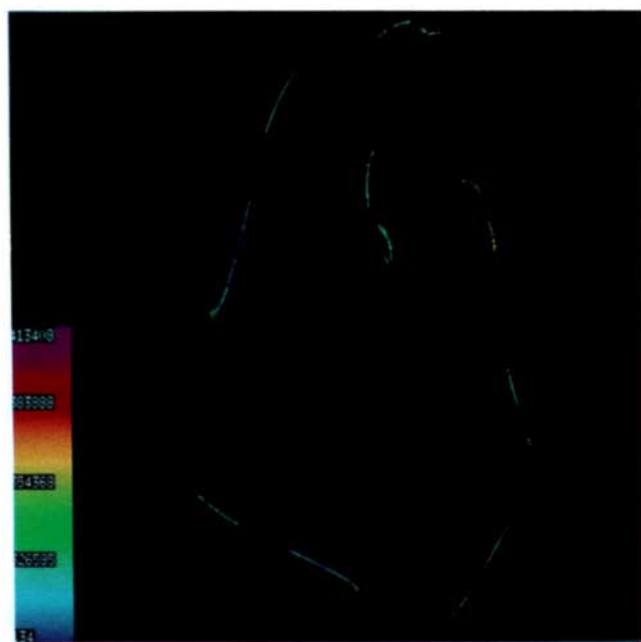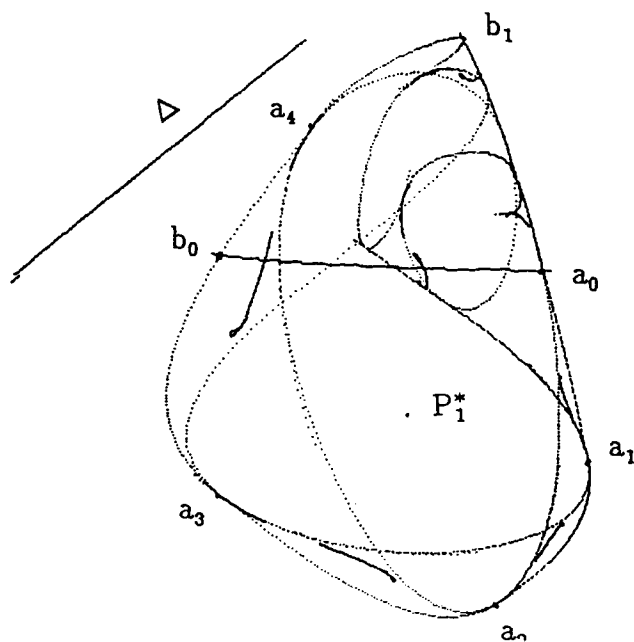
(a)   (b)

Fig. 11.   (a) $\lambda = 0.641$, histogram of the 7.2-band chaotic attractor in the rectangle $[0.5, 1.09] \times [0.14, 0.73]$, $N_1 = 8192$, $N_2 = 1024$; (b) The chaotic attractor inside d_a'.
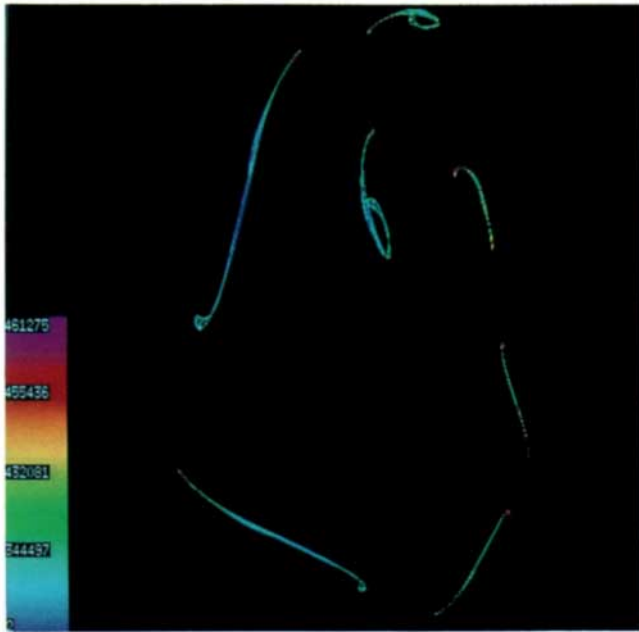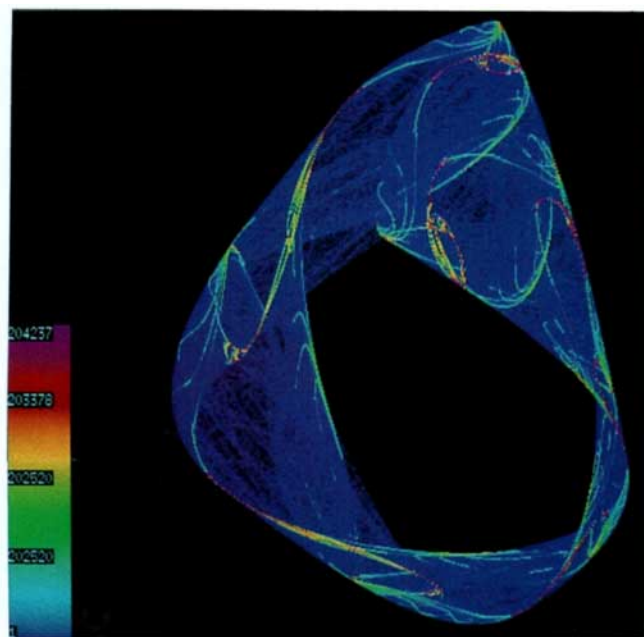
(a)
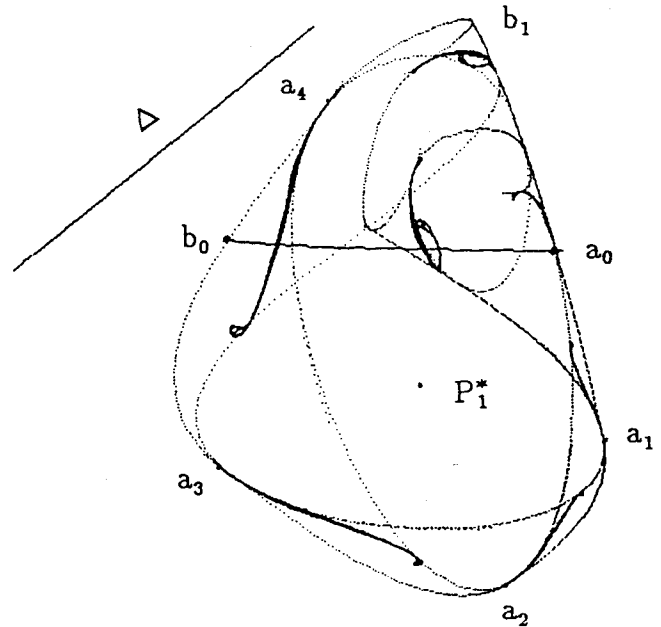
(b)

Fig. 12.   (a) $\lambda = 0.643$, histogram of the 7-band chaotic attractor in the rectangle $[0.5, 1.09] \times [0.14, 0.73]$, $N_1 = 8192$, $N2 = 1024$; (b) The chaotic attractor inside d'_a.

Throughout this work, we give in the color figures (with color scale) the histogram of the attracting set, obtained as follows. After a transient of N_1 iterations, the points of N_2 iterations have been plotted, for each of the $19\,100$ initial conditions (x_0, y_0) in the rectangle $[x\inf, x\sup] \times [y\inf, y\sup]$. The values of N_1 and N_2, and the rectangle of the plane, are reported in the figure captions. The color scale indicates the frequency at which a pixel was hit by an orbit.

The dynamics observed in our example concerning the bifurcations on a closed invariant curve and those initiated from a particular cycle are similar to those described by Mira [1980] in a different example (see also in Gumowski & Mira [1980], pp. 352–356).

The 7.2-band chaotic attractor of Fig. 11 gives rise to the 7-band attractor of Fig. 12 by a global bifurcation which is analogous to the closure of boxes of the second kind in the box-within-a-box bifurcation structure (it involves the 7-cycle saddle existing between each pair of bands).

The global bifurcation which causes the abrupt increase of the chaotic set from that of Fig. 13 to that of Fig. 14 is another contact bifurcation, between the chaotic 7-bands attractor and the boundary of its basin of attraction. This global bifurcation

is analogous to the closure of boxes of the first kind in the box-within-a-box bifurcation structure.

We shall see several other global bifurcations similar to those described above. Let us call them contact bifurcations of the second kind and contact bifurcations of the first kind, involving cyclic chaotic areas d_i. The distinction between these two kinds of contact bifurcation has been made for the first time by Mira, see the exemplary case with several examples in Mira & Narayaninsamy [1992]. From this paper and from Mira [1992] the two bifurcations may be characterized as follows. Let d_i denote a k-cyclic chaotic area (i.e. invariant for the map T^k), $k \geq 1$.

A *contact bifurcation of the second kind* is due to the contact between the boundary of d_i and the boundary of its basin of attraction $\mathcal{D}(d_i)$ at a point belonging to the frontier of the *immediate basin* of another attracting set. If the attracting set on "the other side" is a chaotic area, the contact causes the reunion of chaotic areas.

A *contact bifurcation of the first kind* is due to the contact between the boundary of d_i and the boundary of its basin of attraction $\mathcal{D}(d_i)$ at a point belonging to the frontier of the basin of another attracting set which is *not on the immediate basin*. If the attracting set on "the other side" is a chaotic
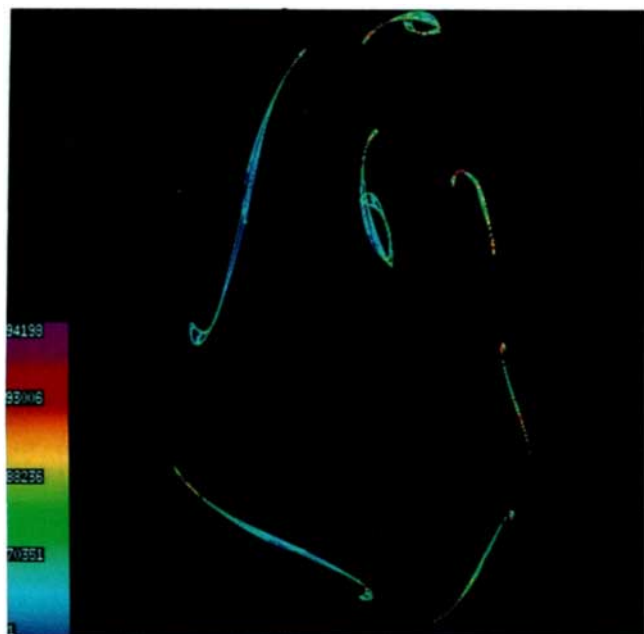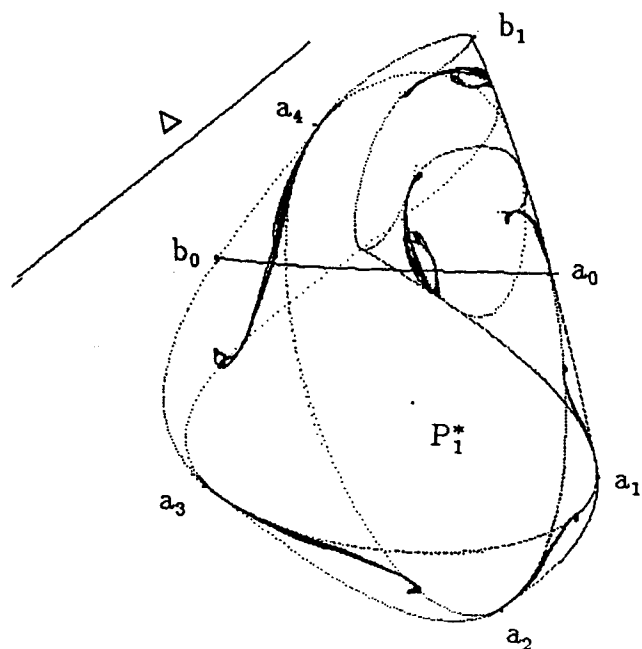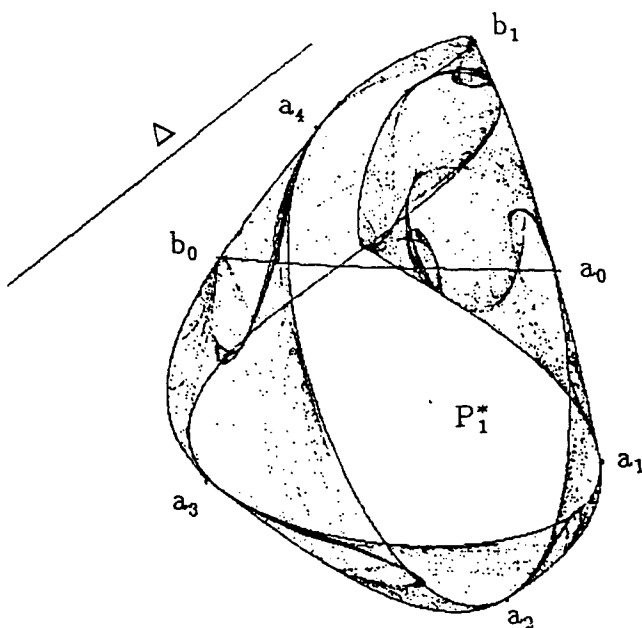
(a)   (b)

Fig. 13.   (a) $\lambda = 0.6439$, histogram of the 7-band chaotic attractor in the rectangle $[0.5, 1.09] \times [0.14, 0.73]$, $N_1 = 8192$, $N2 = 1024$; (b) The chaotic attractor inside d_a'.

(a)   (b)

Fig. 14.   (a) $\lambda = 0.644$, histogram of the chaotic attractor in the rectangle $[0.5, 1] \times [0.13, 0.77]$, $N_1 = 8192$, $N2 = 1024$; (b) The annular chaotic area d_a'.

area, the contact causes the spread into wider chaotic areas (cyclical or not).

Let us consider again the transition from the 7.2-cyclic chaotic attractor of Fig. 11 to the 7-cyclic attractor. The contact between one of the areas of the 7.2-cycle attractor and its basin boundary occurs at a point belonging to the local stable set of the 7-cycle saddle, which separates two immediate basins, giving rise to the reunion of the immediate basins in contact. As this occurs pair by pair, the resulting set is a 7-band chaotic attractor. In Fig. 15(a) is shown an enlargement of a portion of Fig. 11(a). This figure shows two bands of the 7.2-cyclic chaotic attractor near the point V of the
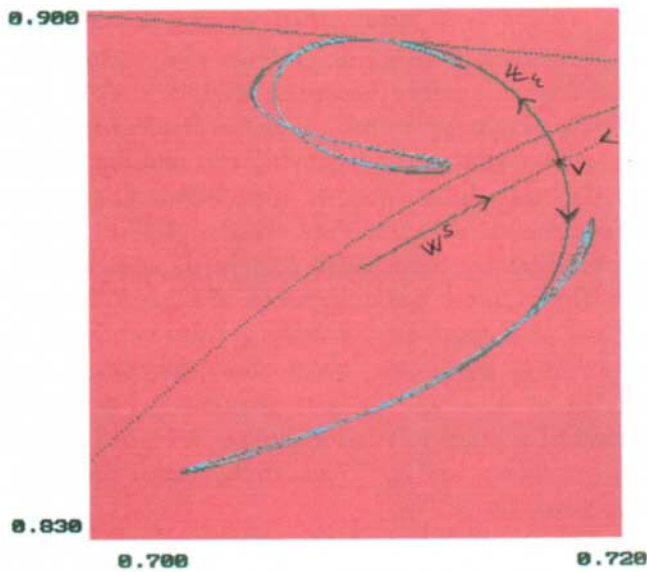
(a) $\lambda = 0.641$
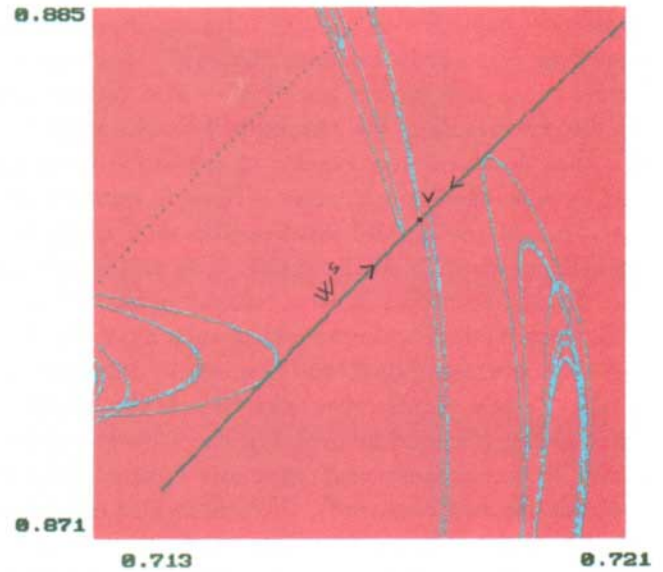
(b) $\lambda = 0.64218$
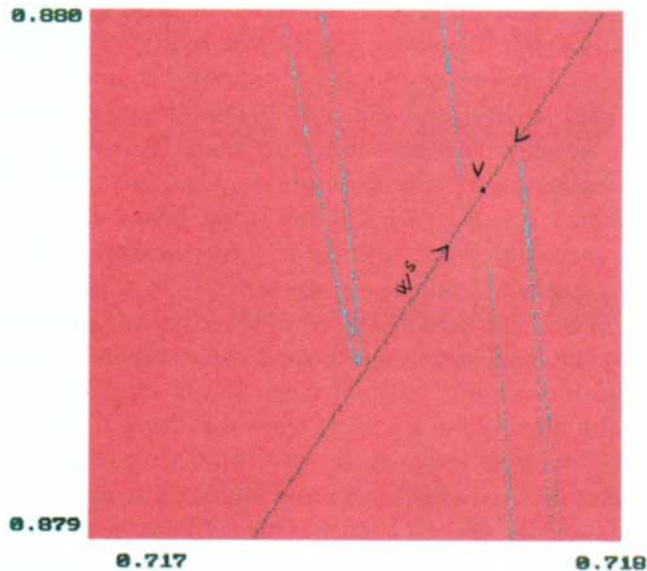
(c) $\lambda = 0.64218$
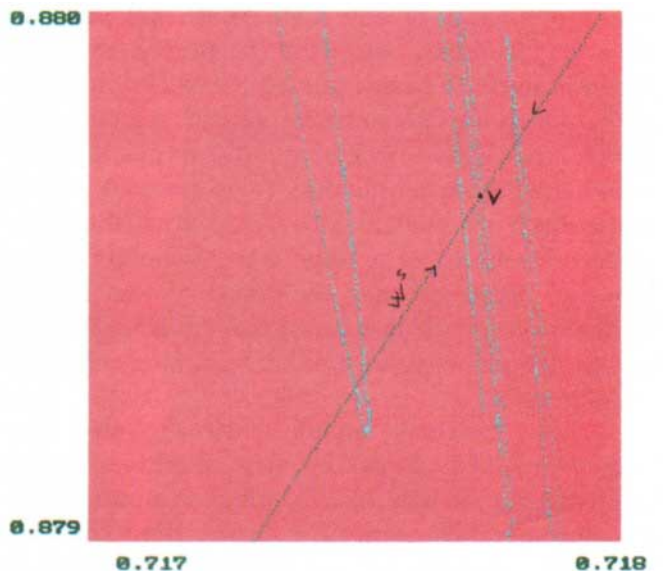
(d) $\lambda = 0.64219$

Fig. 15. (a) $\lambda = 0.641$, enlargement of the 7.2-band attractor of Fig. 11(a) near a point, denoted by V, of the 7-cycle saddle, and portions of the stable set $W^s(V)$ and unstable set $W^u(V)$ of V; (b) $\lambda = 0.64218$, enlargement of the 7.2-band attractor near the stable set $W^s(V)$; (c) $\lambda = 0.64218$, enlargement of the figure in (b) near the saddle point V; there is no contact between the 7.2-band attractor and the stable set $W^s(V)$; (d) $\lambda = 0.64219$, enlargement near the saddle point V, crossing between the 7-band attractor and the stable set $W^s(V)$.

7-cycle saddle of T, together with portions of the stable set $W^s(V)$ (which separates the two branches of the attractor) and the unstable set $W^u(V)$ of V. Increasing λ the two bands come very close to the stable set $W^s(V)$, as it is shown in Fig. 15(b) at $\lambda = 0.64218$. This value of λ is very near the value of contact bifurcation between the chaotic attractor and its basin boundary, as it appears from the enlargement shown in Fig. 15(c) [$W^s(V)$ belongs to the basin boundary]. The value $\lambda = 0.64219$ is already beyond the contact bifurcation value, as shown in Fig. 15(d), because the "old" two chaotic bands cross the stable set of V. The bands are no longer invariant for the map T^{14} but only for T^7, that is, these now belong to the same band of the 7-cyclic chaotic attractor. Thus, a contact bifurcation of the second kind occurs at a value λ_b, $0.64218 < \lambda_b < 0.64219$. At $\lambda = \lambda_b$ the bands of the chaotic attractor have a contact with $W^s(V)$. This example illustrates also that such a contact bifurcation corresponds to the homoclinic bifurcation of the 7-cycle saddle, because before the contact there are no homoclinic orbits of the 7-cycle saddle, while at the contact and after the contact (when the crossing has occurred), the stable and unstable sets of the cycle possess common points.

The basin of attraction of one of the 7 areas, considering the map T^7, becomes very complex. It is formed by an immediate basin and its infinitely many preimages of any rank, which are jumbling in a very complex way with the preimages of the other immediate basins (giving a fuzzy boundary in parts which are accumulation of such disjoint open sets). The contact occurring between one of the 7-band and its basin boundary takes place at a point (or points) not belonging to the frontier of another immediate basin. The same type of contact occurs for each band, so that the result of this contact bifurcation (of the first kind) is an explosion of the seven disjoint chaotic areas into a single annular chaotic area.

This invariant annular chaotic area [see Fig. 14(b)] is bounded by arcs of critical curves, and isolates the hole $H(P_1^*)$, which is an area without any periodic point of T, apart from the fixed point P_1^*. In fact, for any value of λ at which an annular area d_a' exists, it attracts all the points of the immediate basin $\mathcal{D}_{0,1}$ (apart from P_1^*). Inside d_a', we may have two or more coexisting attractors. Although we have not observed this occurrence, it is a generic behavior of nonlinear two-dimensional endomorphisms.

Several bifurcations take place inside the annular absorbing area, while the dynamics on Δ are regular. In fact, S^* is attracting on Δ for $0 < \lambda \le 2/3 = 0.\bar{6}$, while for $0.\bar{6} < \lambda < 0.816$, a 2-cycle $Q_1 - Q_2$ exists on Δ, which is attracting on Δ but a saddle of T for the values of λ which interest us in this regime, that is, for $\lambda < \lambda^*$.

We recall that in this regime two symmetric attractors and basins exist. The bifurcation of both these attractors and basins of attraction occurs at $\lambda = \lambda^*$ ($\lambda^* \simeq 0.7029$) when an arc of the critical curve $a_3a_4 \in LC_{3,a}$ on the boundary of the annular absorbing area becomes tangent to Δ at the periodic point Q_1. Thus, a contact bifurcation of the second kind occurs, causing the reunion of the two disjoint annular chaotic areas into a single connected chaotic area [see Figs. 16(a) and 16(c) before the bifurcation, Figs. 16(b) and 16(d) after the bifurcation]. In the magnifications of Fig. 17, several images of a small arc of $LC_{-1,a}$ (also reported in that figure) are shown, which show the contact occurring at $\lambda = \lambda^*$. A critical point r_3, image of rank-4 of a point r_{-1} belonging to the small arc of $LC_{-1,a}$ shown in Fig. 17(a), merges into the periodic point Q_1.

The points Q_1 and Q_2 of the 2-cycle belong to the area of branching points δ_1, so that this area contains some points whose infinite sequence of preimages under the local inverse, which gives points above $LC_{-1,a}$, converge to the 2-cycle. That is, a local stable set of the 2-cycle saddle exists for the local inverse of T in δ_0. Moreover, the point r_{-1} defined above also belongs to δ_1, and starting from r_{-1} we may construct infinitely many sequences of preimages in d_a'. For example, r_{-1} has two distinct preimages, one in δ_0 and the other below $LC_{-1,a}$, for each new point we take all its preimages in d_a', creating new branches whenever we get a point in the branching area δ_1. If one of these preimages falls into the local stable set of the 2-cycle saddle for the local inverse of T in δ_0 (which is the unstable set of the 2-cycle for T), then we would have a homoclinic orbit of the 2-cycle. We conjecture that this indeed occurs at $\lambda = \lambda^*$, and homoclinic orbits of the 2-cycle $\{Q_1, Q_2\}$ exist. Our conjecture may be numerically verified; in Fig. 17(d) are shown images of rank-i, for i from 1 to 100, of points taken on a small arc of the local unstable set issuing from Q_1 [the direction of which is $(1, -1)$], and we can see points mapped by T above the line Δ, which means that the unstable set of the 2-cycle intersects the stable set of the same cycle on Δ, creating homo-
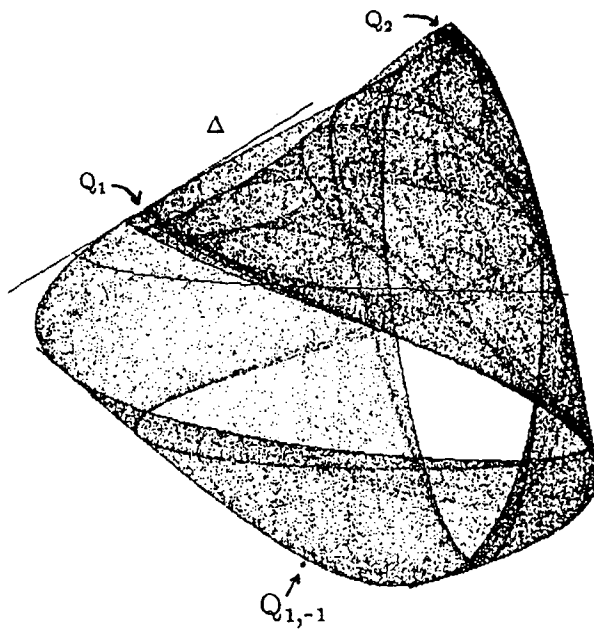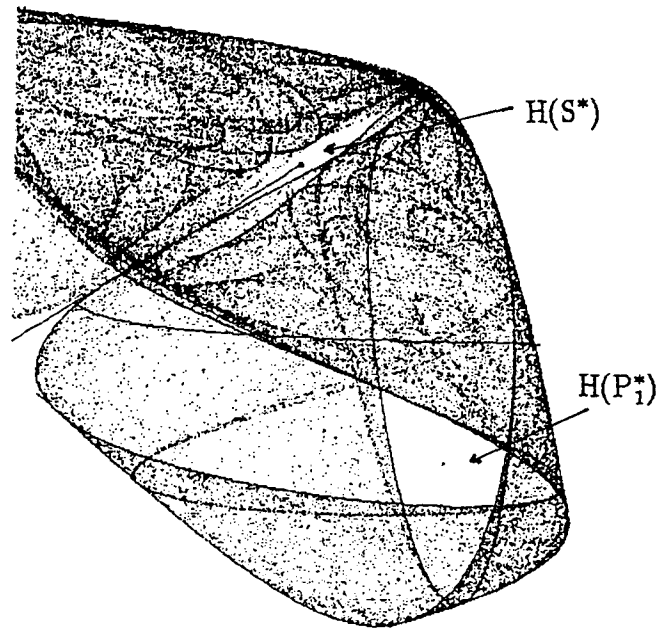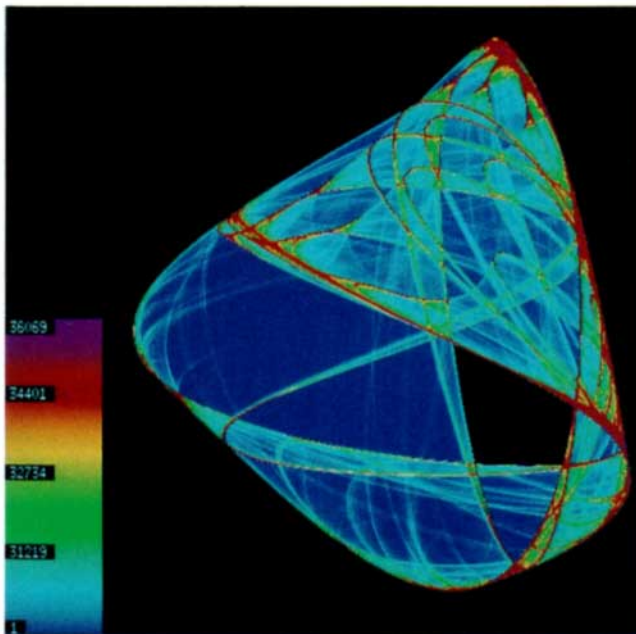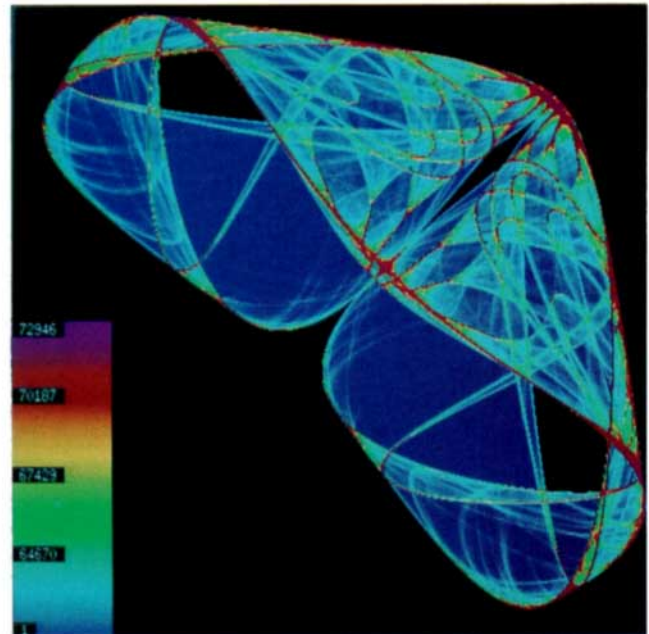
(a) $\lambda = 0.702$

(b) $\lambda = 0.703$

(c) $\lambda = 0.702$

(d) $\lambda = 0.703$

Fig. 16. (a) $\lambda = 0.702$, annular chaotic area d'_a below the diagonal Δ; (b) $\lambda = 0.703$, a portion of the connected chaotic area; (c) $\lambda = 0.702$, histogram of the annular chaotic attractor in the rectangle $[0.4, 1] \times [0.05, 0.9]$, $N_1 = 4096$, $N_2 = 1024$; (d) $\lambda = 0.703$, histogram of the connected chaotic attractor in the square $[0.07, 1] \times [0.07, 1]$, $N_1 = 4096$, $N_2 = 1024$.

clinic points. This implies the existence of infinitely many repelling cycles near the 2-cycle on Δ, cycles which do not belong to Δ, but having Q_1 and Q_2 as accumulation points. This may also be the reason for the density of the points of a trajectory

in these regions, as observed by numerical computations. The main difficulty in proving the existence of homoclinic orbits in this case (as well as in the case shown in Fig. 15) is due to the fact the the cycle is a saddle. We shall see that in a
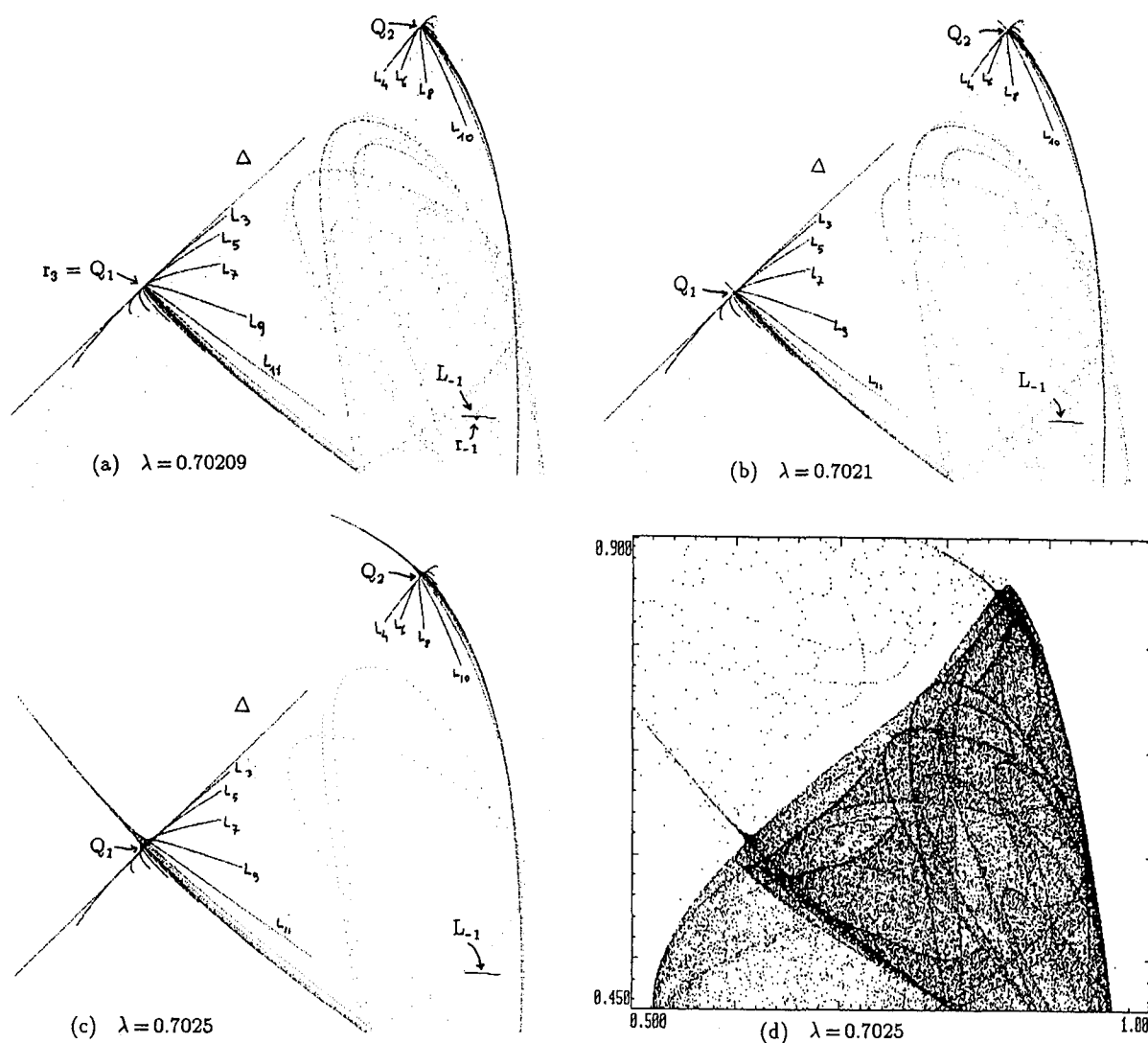
Fig. 17.   (a) $\lambda = 0.70209$, several images of the small arc of $LC_{-1,a}$ denoted by L_{-1}; (b) $\lambda = 0.7021$; and (c) $\lambda = 0.7025$, where the images of the small arc L_{-1} of $LC_{-1,a}$ cross Δ; (d) $\lambda = 0.7025$, images of rank-i, for i from 1 to 100, of 2000 points taken on a small germ (of length 0.0001) of the local unstable set issuing from Q_1.

similar bifurcation involving repelling nodes or repelling foci (the SBR bifurcations of S^* and of the fixed points P_1^*, P_2^*, in the next section), the existence of infinitely many homoclinic orbits is easier to prove.

6.   Dynamics of T in the Fourth Regime

After the contact bifurcation at $\lambda = \lambda^*$ the two disjoint attractors (for $\lambda < \lambda^*$) become one single attractor (for $\lambda > \lambda^*$) inside a unique absorbing area d' (simply connected), which is always bounded by the images of an arc of $LC_{-1,a}$, which is now the arc a_0a_0', where a_0' is the symmetric image of a_0

with respect to Δ (a_0 and a_0' are the two points of intersection between $LC_{-1,a}$ and LC_a).

An example is shown in Fig. 18. Figure 18(a) shows the simply connected absorbing area d' and Fig. 18(b) shows the chaotic area d contained in d'. It may be noted that the chaotic area d is connected but not simply connected. Three holes exist inside d', one surrounding the fixed point S^* (which is now a repelling node), say $H(S^*)$, the other two, $H(P_1^*)$ and the symmetric $H(P_2^*)$, are around the fixed points P_1^* and P_2^* (repelling foci). The boundaries of these holes consist of critical arcs belonging to the images of the arc a_0a_0'.

The hole $H(S^*)$ disappears at the SBR bifurcation of S^*, at $\lambda = \lambda_s \simeq 0.714$ (see Fig. 19). At this
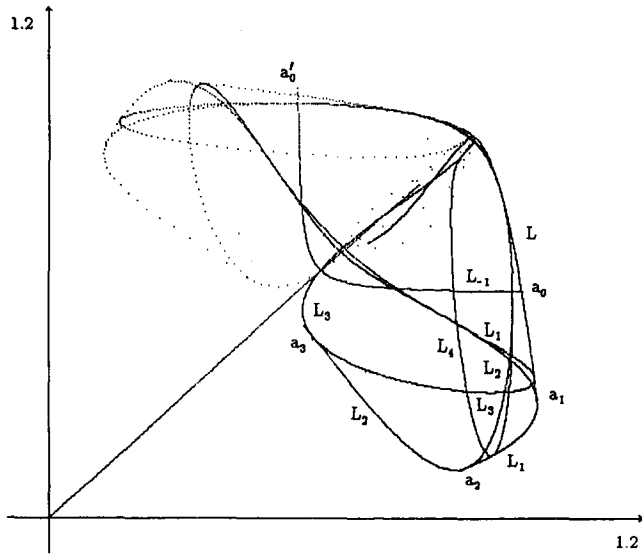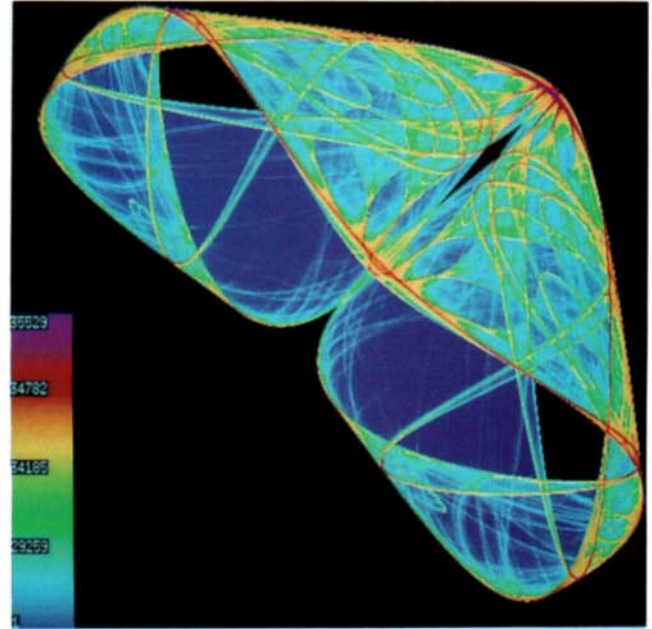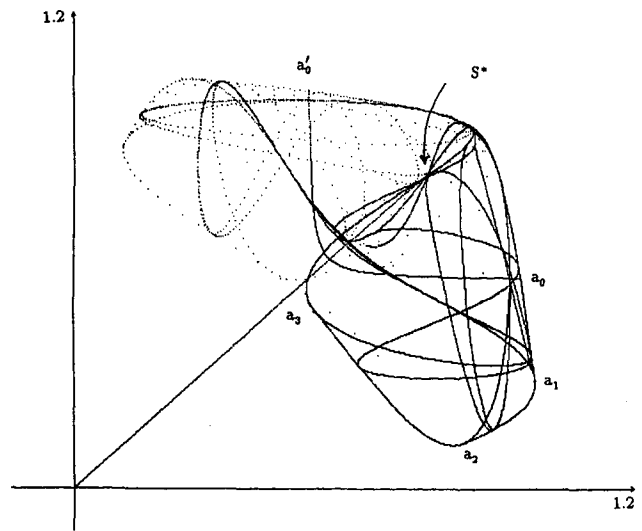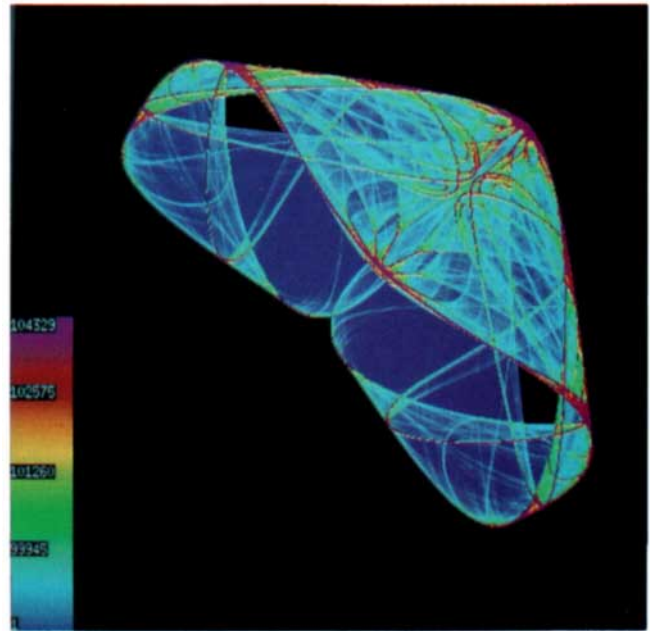
(a) $\lambda = 0.705$ (b) $\lambda = 0.705$

Fig. 18. $\lambda = 0.705$. (a) The absorbing area d'; (b) histogram of the chaotic attractor in the square $[0.07, 1] \times [0.07, 1]$, $N_1 = 4096$, $N_2 = 1024$.

(a) $\lambda = 0.714$ (b) $\lambda = 0.714$

Fig. 19. $\lambda = 0.714$. (a) The absorbing area d'; (b) histogram of the chaotic attractor in the square $[-0.1, 1.1] \times [-0.1, 1.1]$, $N_1 = 4096$, $N_2 = 1024$.

bifurcation value, the two symmetric rank-1 preimages of S^* outside Δ fall on the boundary of d', and thus on an arc of a critical curve. All the critical curves $LC_{i,a}$ for $i \geq 3$ pass through S^* [some are shown in Fig. 19(a)]. This means that at $\lambda = \lambda_s$ a point belonging to the portion of $LC_{-1,a}$ below Δ, say r_{-1}, has an image, say r_k, which merges into S^* (and a symmetric point exists, say r'_{-1}, belonging to the portion of $LC_{-1,a}$ above Δ, such that $r'_k = S^*$). Taking the infinitely many sequences of preimages of r_{-1} contained in d', we can see that many points will fall in a neighborhood of S^* in which the local inverse giving points above $LC_{-1,a}$ is a contraction (having an attracting node in S^*). This process illustrates the infinitely many homoclinic orbits of S^* existing after the SBR bifurcation, which persist for any value of $\lambda > \lambda_s$. This is due to the fact that S^* remains an attracting node for the local inverse above $LC_{-1,a}$, for any $\lambda > \lambda_s$, and its rank-1 preimage below $LC_{-1,a}$ belongs to d', so that we may construct the sequences of preimages starting from S^* obtaining points in a suitable neighborhood of S^*. We recall [Marotto, 1978; Gardini, 1992a] that to each homoclinic orbit are associated infinitely many repelling cycles of T, which belong to Cantor sets of points invariant for some power of T. Note however

that this bifurcation is not the SBR bifurcation of the fixed point S^* for the restriction of T on Δ (this will occur later at a greater value of λ), so that none of the infinitely many periodic points of T near S^* belong to Δ.

After the SBR bifurcation of S^* the absorbing area d' is connected with two holes, $H(P_1^*)$ and $H(P_2^*)$. These holes decrease on increasing λ and disappear at the SBR bifurcation of the fixed points P_1^* and P_2^*, which occurs at $\lambda = \lambda_p \simeq 0.737$ (in Fig. 20 we can observe the critical curves $LC_{i,a}$ for $i \geq 1$ passing through the fixed point P_1^*). We may repeat the same reasoning as above, with the difference that we consider the local inverse of T which gives points in d' below $LC_{-1,a}$, for which the fixed points P_1^* and P_2^* are attracting foci for any value of $\lambda > \lambda_p$. It follows that P_1^* and P_2^* are snap-back repellers for $\lambda > \lambda_p$ (with all that this statement implies about the dynamics of T).

After the SBR bifurcation of P_1^* and P_2^*, the chaotic area d coincides with d' and is simply connected [see Figs. 20(b) and 21(a)]. Let us make an observation on the chaotic area $d \subseteq d'$ (with d simply connected or not). As we have seen in several figures, the generic trajectory that we observe numerically is often chaotic, but this does not mean
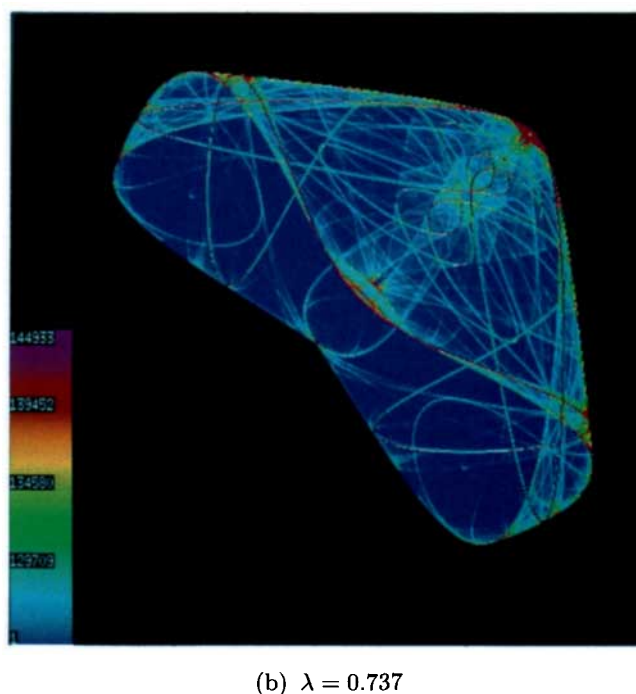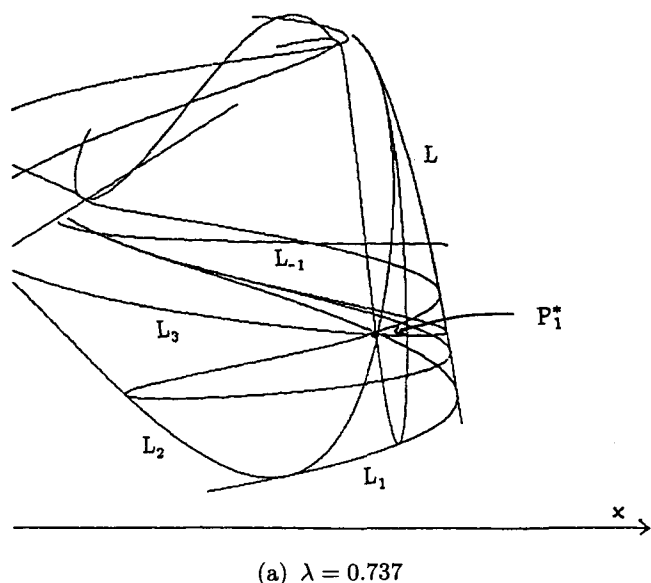

(a) $\lambda = 0.737$

(b) $\lambda = 0.737$

Fig. 20. $\lambda = 0.737$. (a) Portion of the absorbing area d'; (b) histogram of the chaotic attractor in the square $[-0.1, 1.1] \times [-0.1, 1.1]$, $N_1 = 4096$, $N_2 = 1024$.

that in this area there are no stable cycles. Attracting cycles may exist (and we conjecture that they do) with small basins of attraction, having a complex shape and fuzzy boundaries (on which the dynamics of T are chaotic). That is, unstable chaos is likely to occur, and the trajectories observed in these chaotic regimes are due to truncation errors.

Up to now, T has been studied as if it were a map having only 0 or 2 preimages of rank-1. This is because the invariant area d' has void intersection with the branch $LC_{-1,b}$, so that the fact that T is a map with 0, 2 or 4 preimages of rank-1 has only influenced the construction of the basin of attraction of the absorbing areas. However, as is shown in Fig. 21(a), now the branch $LC_{-1,b}$ is quite near the invariant area d', and we shall see that the influence of the 0-2-4 character of the inverses of T comes to play some role now, as also before, at lower values of λ.

We have observed a decrease in the "chaoticity" of the trajectories inside d' as it approaches $LC_{-1,b}$. This may be explained by sequences of reverse flip and fold bifurcations which make previously existing cycles disappear (that is, attracting $2k$-cycles disappear by reverse flip-bifurcation leaving an attracting k-cycle, previously repelling; or a couple of two k-cycles disappear via reverse fold-bifurcation). Such a process can easily be observed in one-dimensional endomorphisms, for example in cubic maps or in bimodal maps without symmetry (several examples are shown in Gardini & Lupini [1992]). A similar process (i.e. reverse bifurcations) occurs also in two-dimensional endomorphisms. In our opinion, in this example it begins when the excess preimage curves of $LC_{-1,b}$, that is $LC^{e1}_{-1,b}$ and $LC^{e2}_{-1,b}$, have a contact and then intersect the invariant area d'. This contact occurs at a value of λ in the previous regime. Moreover, noting that the
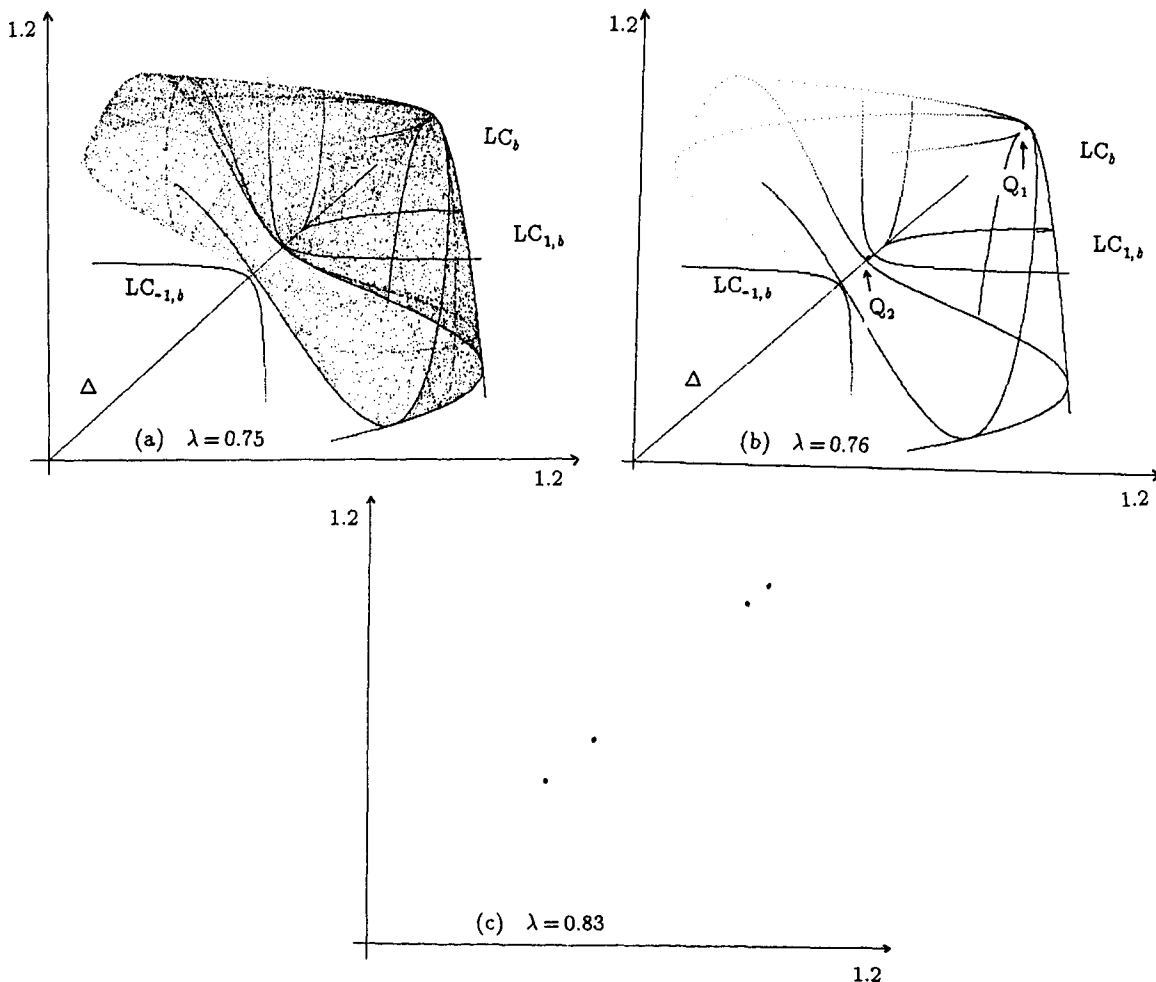

Fig. 21. (a) $\lambda = 0.75$ chaotic area d'; (b) $\lambda = 0.76$, attracting node $Q_1 - Q_2$ on Δ, in the absorbing area d'; (c) $\lambda = 0.83$, attracting 2^2-cycle on Δ.

images of the area of d' crossed by the excess preim-
ages are mapped by T to points near Δ and near the
2-cycle $Q_1 - Q_2$, we may explain the disappearance
of periodic points outside Δ, near the 2-cycle on Δ.
These disappearances are however compensated by
the increase of cycles with periodic points near the
other three fixed points of T (S^*, P_1^* and P_2^*) and
their SBR bifurcations.

At $\lambda \simeq 0.76$, the 2-cycle on Δ becomes an at-
tracting node of T [Fig. 21(b)] and, even if d' con-
tains infinitely many repelling chaotic sets (as S^*,
P_1^* and P_2^* are SBRs), the generic trajectory nu-
merically observed converges to the attracting cy-
cle $Q_1 - Q_2$. Now a neighborhood of this 2-cycle
exists containing no periodic points of T, and the
preimages of this neighborhood give the basin of at-
traction of the 2-cycle, which has certainly a very
complex shape, with a fuzzy boundary.

The disappearance of cycles in a neighborhood
of $Q_1 - Q_2$ described above shows that the 0-2-4
character of the inverses of T influences the dy-
namics of T before the contact of d' with $LC_{-1,b}$
(through the effect of the excess preimage curves).
However, the main influence on the dynamics of T
takes place after the contact (and then intersection)
of d' with $LC_{-1,b}$. This is because points of d' be-
low $LC_{-1,b}$ are mapped by T in a region (bounded
by critical arcs of some $LC_{i,a}$ and an arc of LC_b)
containing points having four distinct preimages of
rank-1 inside d' itself. From now on, when chaotic
dynamics are observed, this region is the one more
frequently visited by the points of a trajectory.

The flip-bifurcation of the 2-cycle in Δ is the
one due to the logistic map g_λ on Δ itself. A stable
2^2-cycle in Δ is observed in Fig. 21(c). This 2^2-
cycle however becomes repelling (in the direction
transverse to Δ) due to the two-dimensional char-
acter of T, as it undergoes a flip bifurcation due to
the eigenvalue related to the eigenvector transverse
to Δ. In Fig. 22(a) an attracting 8-cycle is shown
which does not belong to Δ; the 2^2-cycle on Δ
is attracting for the logistic map g_λ, but is a saddle
of T.

Considering the points of the 8-cycle as fixed
points of the map T^8 we can repeat the same ob-
servations made for the fixed point P_1^* of T:

— the points of the cycle undergo a Neimark–Hopf
  bifurcation which gives rise to 8 closed invariant
  curves [Fig. 22(b)];
— chaotic sets and a contact bifurcation of the sec-
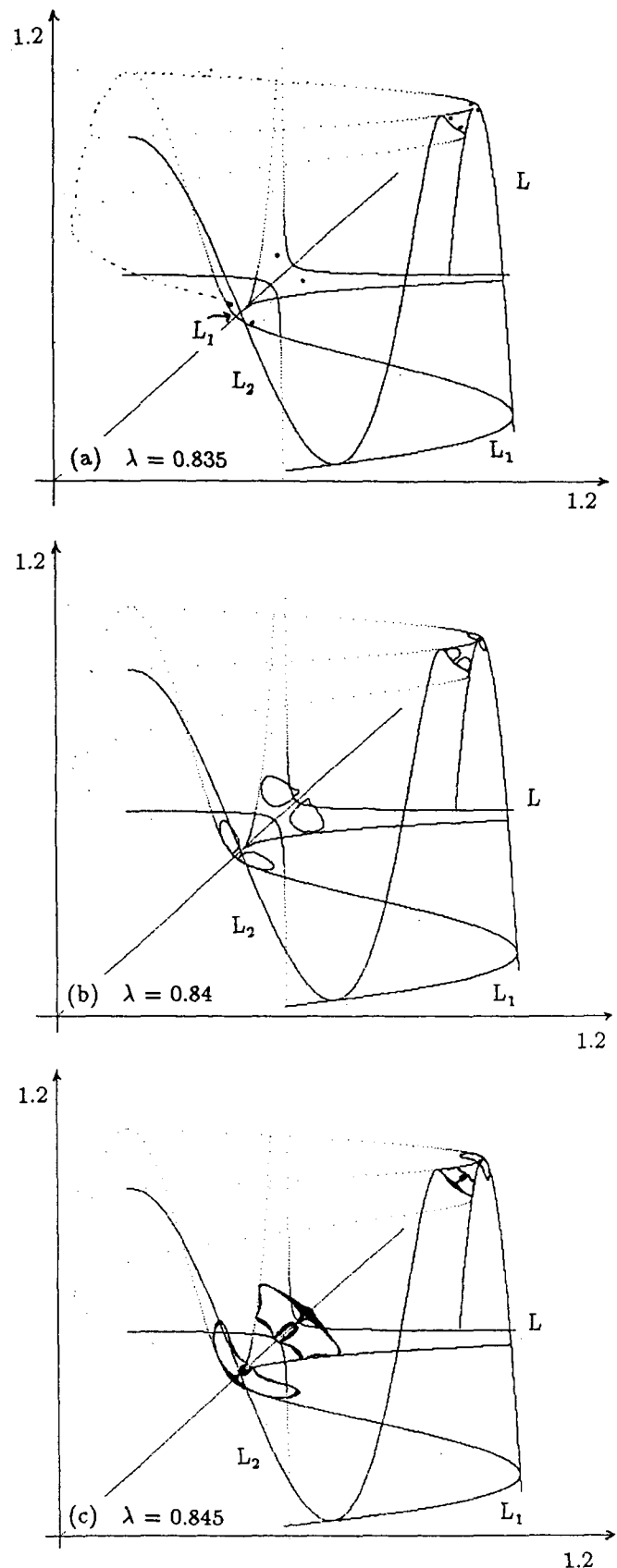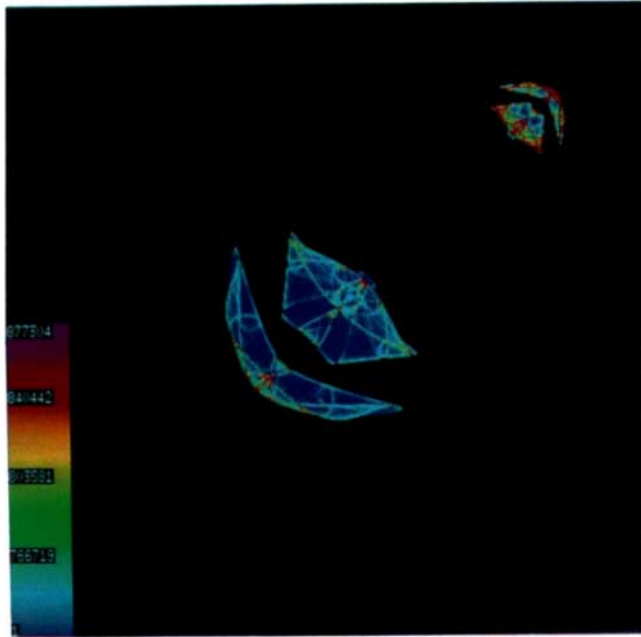 ond kind produce a 4-cyclic annular chaotic area
  [Fig. 22(c)];

Fig. 22.   Attracting sets inside the absorbing area d'.
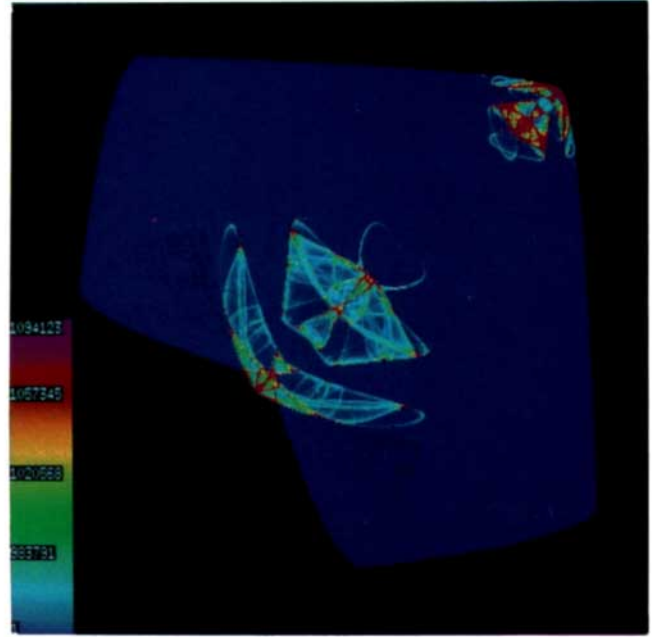(a) $\lambda = 0.835$; (b) $\lambda = 0.84$; (c) $\lambda = 0.845$.

— some SBR bifurcation gives a 4-cyclic chaotic area, not annular [Fig. 23(a)];

— contact bifurcation of the first kind between the 4 basins of attraction and the 4-cyclic chao-

tic areas gives rise to a single observed chaotic attractor in the absorbing area d' $(d = d')$ [Figs. 23(b) and 23(c)].
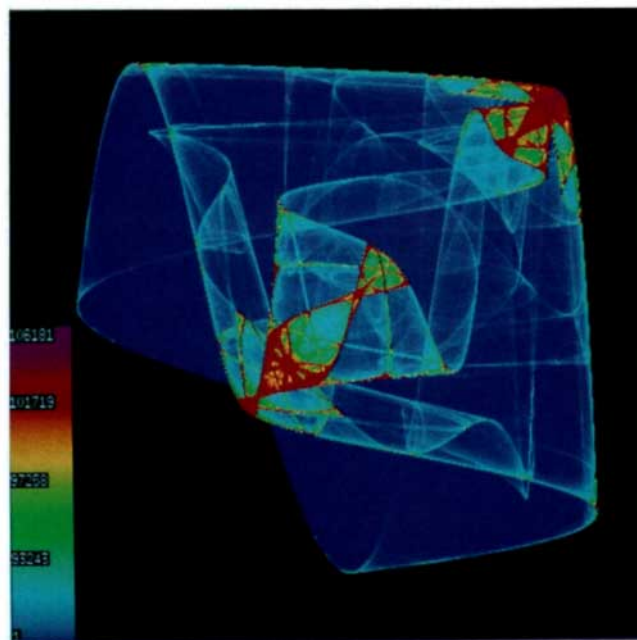
In Fig. 24(a) an attracting 4-cycle of T is shown,

(a) $\lambda = 0.852$

(b) $\lambda = 0.854$

(c) $\lambda = 0.865$

Fig. 23.   Histograms of the attracting sets in the square $[-0.1, 1.1] \times [-0.1, 1.1]$, $N_1 = 1024$, $N_2 = 1024$. (a) $\lambda = 0.852$; (b) $\lambda = 0.854$; (c) $\lambda = 0.865$.
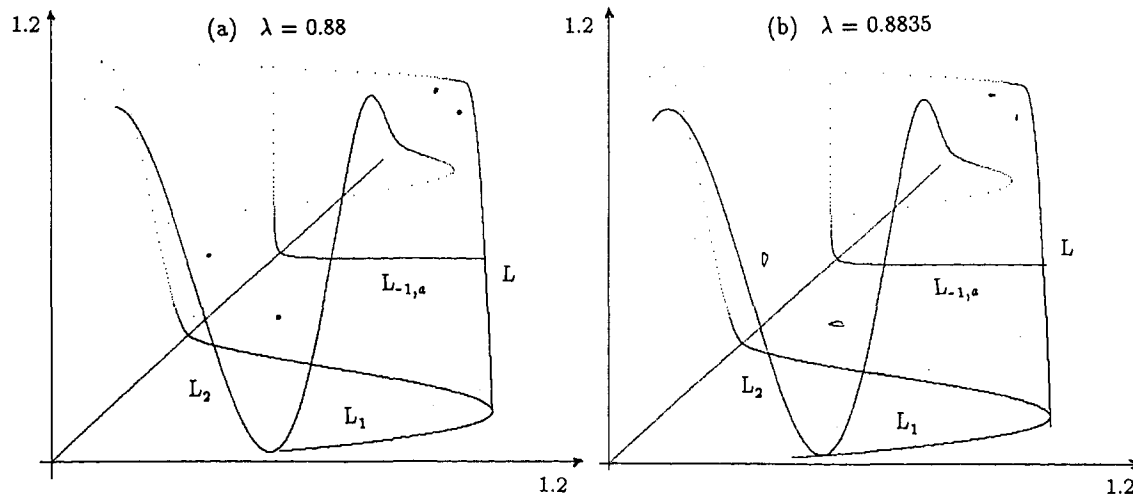
Fig. 24.   Attracting sets inside the absorbing area d'. (a) $\lambda = 0.88$; (b) $\lambda = 0.8835$.

for which we repeat the sequence:

— it bifurcates via Neimark–Hopf giving rise to 4 closed invariant curves [Fig. 24(b)];
— periodic orbits on the closed curves can be seen and then again closed curves followed by transition into 4-cyclic annular chaotic areas [Fig. 25(a), with a magnification in Fig. 25(b)];
— contact bifurcation of the first kind giving rise to a unique observed chaotic attractor in the absorbing area d' ($d = d'$) [Fig. 25(c) with a magnification in Fig. 25(d)].

On Δ, g_λ has an attracting 2^2-cycle in Fig. 22, an attracting 2^3-cycle in Figs. 23(a) and 23(b), 2-cyclic absorbing intervals in Figs. 23(c), 24 and 25. All the repelling cycles on Δ are saddles of T.

Now that the dynamics on Δ are also chaotic (i.e. for $\lambda > \lambda_{1s} \simeq 0.8566$), the SBR bifurcation of S^* for the restriction of T on Δ, that is for g_λ, is approached. At $\lambda = 0.89$ [see Fig. 26(a)] the two critical curves $LC_{2,a}$ and $LC_{3,a}$ intersect Δ at the two points c_2 and c_3 which are near the fixed point S^*. The SBR bifurcation of S^* for g_λ occurs when the two critical curves $LC_{2,a}$ and $LC_{3,a}$ intersect Δ at the fixed point $c_2 = c_3 = S^*$ (at $\lambda = \lambda_{21}^* \simeq 0.8928$). Before this, all the points homoclinic to S^* in d' were outside Δ. After, there are points homoclinic to S^* also in Δ.

It seems that the bifurcation mechanism which governs the "route to chaos" of the two-dimensional map T is not related to that of the one-dimensional

logistic map g_λ, or is only partly related because it is due to bifurcations which are typical of the two-dimensional map, at least for values of λ below λ_{1s}. However, increasing the parameter λ, the analogy with the one-dimensional case (logistic map) seems to become more adequate. The chaotic area d (equal to d') tends to become a unit square (see Fig. 26), that is, approaches the boundary of its basin of attraction. At $\lambda = 1$ the SBR bifurcation of the fixed point at the origin O occurs, and $d = d' = \mathcal{D}$ is exactly the unit square (the vertices of the unit square are the distinct preimages of the origin). It is an invariant chaotic area but is not absorbing (a neighborhood U of d' does not exist because the expanding fixed point O belongs to the boundary of d'). At $\lambda = 1$, T is chaotic in the unit square in the precise sense of the term (that is, no attracting cycle may exist, all the possible cycles of T have been created and all are repelling). In fact, the map T^2 reduces to two disjoint equations, two squared logistics without interaction: $T^2(x, y) = (f^2(x), f^2(y))$ where $f(x) = 4x(1 - x)$. LC_{-1} becomes the pair of straight lines $x = 1/2$ and $y = 1/2$; LC, the straight lines $y = 1$ and $x = 1$; LC_1, the lines $x = 0$ and $y = 0$ [see Fig. 26(f)]. At $\lambda = 1$, g_λ is chaotic on the segment $[c_1, c] = [0, 1]$ on Δ.

At $\lambda = 1$ the last contact bifurcation of d' occurs. It is a homoclinic bifurcation (SBR of the origin). This is a particular contact bifurcation of the first kind. The difference from those previously seen is that the attractor "on the other side" of the
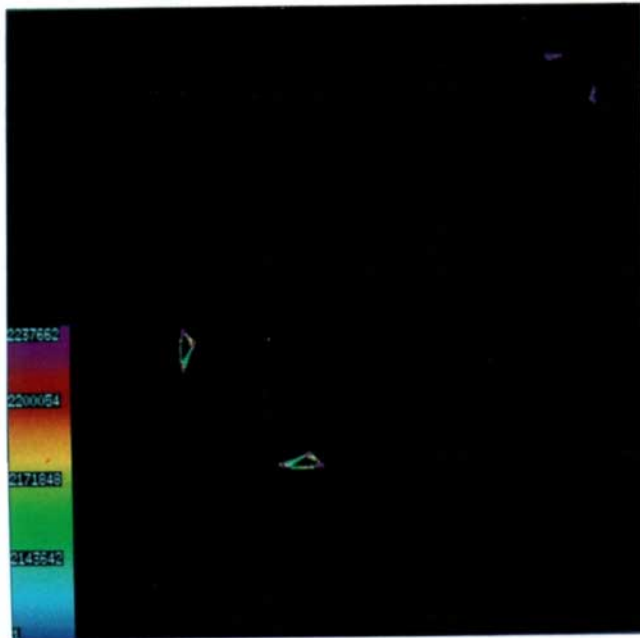
(a) $\lambda = 0.88498$
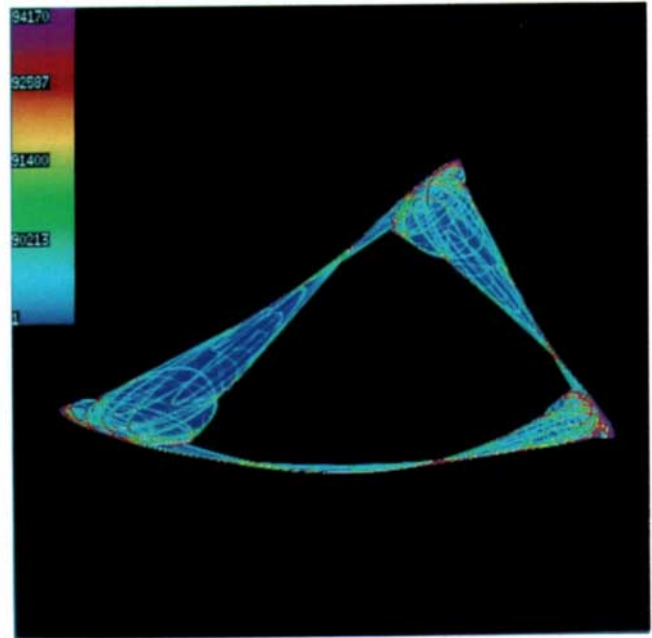

(b)
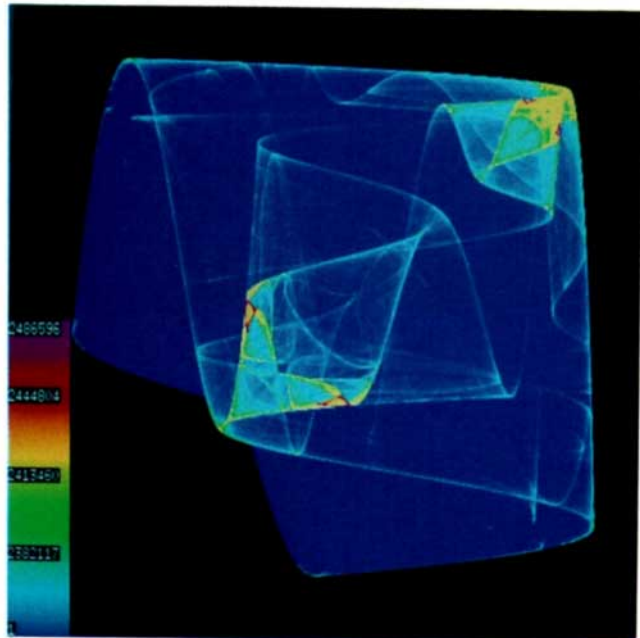
(c) $\lambda = 0.88499$
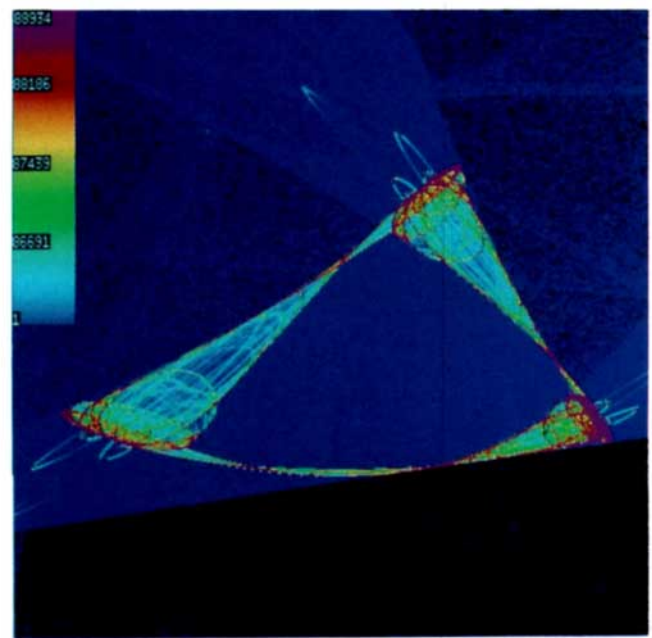
(d)

Fig. 25.   Histograms of the attracting sets. (a) $\lambda = 0.88498$, 4-cyclic annular chaotic areas in the square $[0.1, 1.1] \times [0.1, 1.1]$; (b) enlargement of the portion of (a) in the rectangle $[0.474576, 0.546674] \times [0.332147, 0.375085]$, $N_1 = 4096$, $N_2 = 1024$; (c) $\lambda = 0.88499$ histogram of the attracting set in the square $[-0.1, 1.1] \times [-0.1, 1.1]$; (d) enlargement of the portion of (c) in the rectangle $[0.474576, 0.546674] \times [0.332147, 0.375085]$, $N_1 = 8192$, $N_2 = 2048$.

basin is a point at infinity (instead of an attractor at finite distance), so that it will have the catastrophic effect of a disappearance of the bounded chaotic attractor.
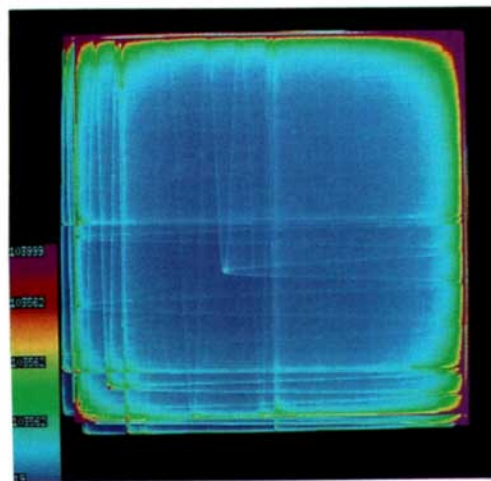
For $\lambda > 1$, the unique attractor is a point at infinity. In the unit square there survives a Cantor set Λ, invariant for T, with repelling cycles, that is, a "strange repeller."
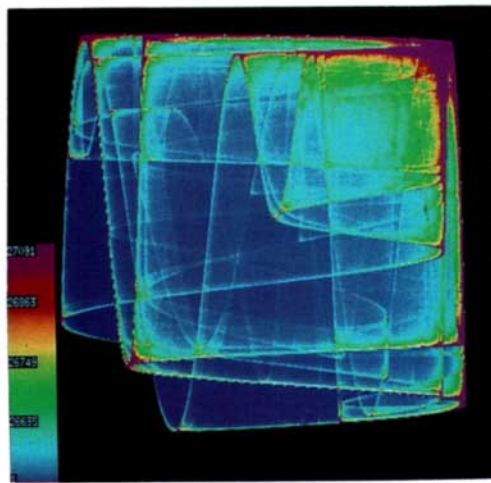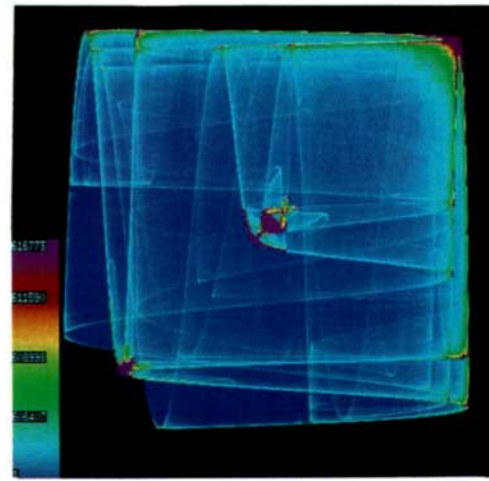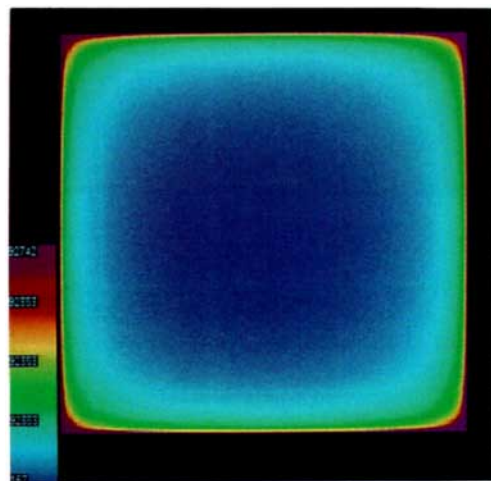
(a) $\lambda = 0.89$
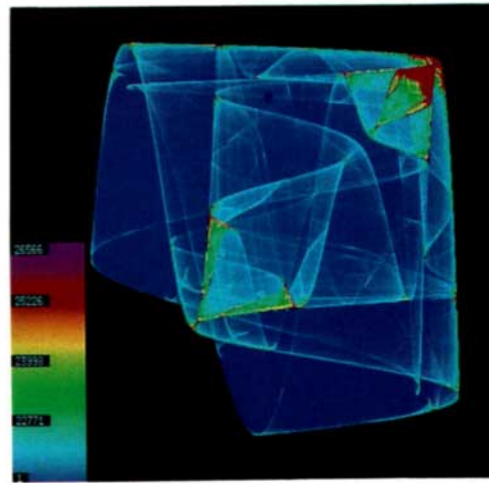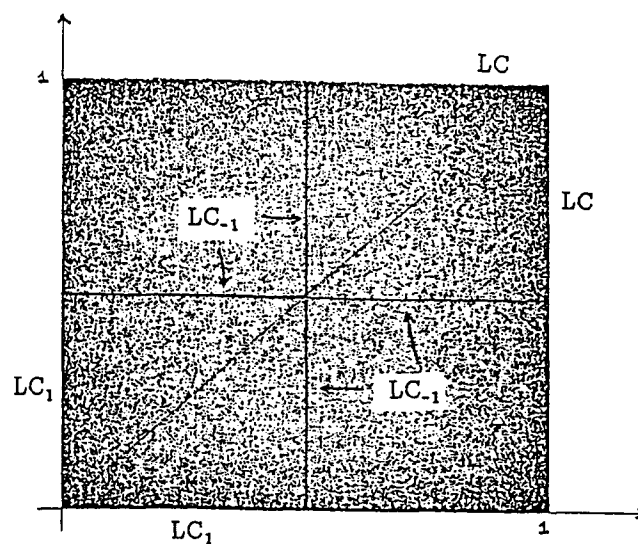

(b) $\lambda = 0.94$

(c) $\lambda = 0.95$

(d) $\lambda = 0.99$

(e) $\lambda = 0.9999$

(f) $\lambda = 0.9999$

Fig. 26. Histograms of chaotic attractors. $N_1 =$ '1024, $N_2 = 512$. (a) $\lambda = 0.89$, in the square $[-0.1, 1.1] \times [-0.1, 1.1]$; (b) $\lambda = 0.94$; (c) $\lambda = 0.95$; (d) $\lambda = 0.99$; (e) $\lambda = 0.9999$, in the square $[-0.125, 1.075] \times [-0.125, 1.075]$; (f) a chaotic trajectory in the unit square at $\lambda = 0.9999$.

Acknowledgments

References

Aicardi, F. & Invernizzi, S. [1992] "Memory effects in discrete dynamical systems," *Int. J. Bifurcation and Chaos* **2**(4), 815–830.

Barugola, A. [1984] "Quelques propriétés des lignes critiques d' une récurrence du second ordre à inverse non unique. Determination d' une zone absorbante," *R.A.I.R.O. Numerical Analysis* **18**, 137–151.

Barugola, A. [1986] "Sur certains zones absorbantes et zones chaotiques d'un endomorphisme bidimensionnel," *Int. J. Non-Linear Mechanics* **21**, 165–168.

Barugola, A., Cathala, J. C. & Mira, C. [1986] "Annular chaotic areas," *Nonlinear Analysis, T.M. & A.* **10**, 1223–1236.

Barugola, A. & Cathala, J. C. [1992] "An extension of the notion of chaotic area in two-dimensional endomorphisms," *Proceedings of the European Conference on Iteration Theory* (Batschuns, Austria, Sept. 1992), in press.

Cathala, J. C. [1983] "Absorptive area and chaotic area in two-dimensional endomorphisms," *Nonlinear Analysis, T.M. & A.* **7**, 147–160.

Cathala, J. C. [1987] "Bifurcations occurring in absorptive and chaotic areas," *Int. J. of Systems Sci.* **18**, 339–349.

Cathala, J. C. [1990] "Multi-connected chaotic areas in second order endomorphisms," *Int. J. of Systems Sci.* **21**, 863–887.

De Sousa Vieira, M., Lichtenberg, A. J. & Lieberman, M. A. [1991] "Nonlinear dynamics of self-synchronizing systems," *Int. J. Bifurcation and Chaos* **1**(3), 691–699.

Devaney, R. L. [1989] *An Introduction to Chaotic Dynamical Systems* (Addison-Wesley, Reading).

Gaertner, W. & Jungeilges, J. [1992] "A model of interdependent consumer behavior: Nonlinearities in $\mathbb{R}^2$," in *Proceedings Conf. on Mathematical Economics*, (Certosa, Siena, Italy, April 1991) eds. Gori, F. & Geronazzo, L. (Springer-Verlag, 1993).

Gardini, L. [1991] "Global analysis and bifurcations in two-dimensional endomorphisms by use of critical curves," in *European Conference on Iteration Theory*, eds. Lampreire, Llibre, Mira, Sousa Ramos & Targonski (World Scientific, Singapore).

Gardini, L. [1992a] "Homoclinic bifurcations in n-dimensional endomorphisms due to expanding periodic points," *Nonlinear Analysis, T.M. & A.* (to appear).

Gardini, L. [1992b] "Homoclinic orbits of saddles in two-dimensional endomorphisms," *Proceedings of the European Conference on Iteration Theory* (Batschuns, Austria, Sept. 1992), in press.

Gardini, L., Cathala, J. C. & Mira, C. [1992] "Contact bifurcations of absorbing areas and chaotic areas in two-dimensional endomorphisms," *Proceedings of the European Conference on Iteration Theory* (Batschuns, Austria, Sept. 1992), in press.

Gardini, L. & Lupini, R. [1992] "One-dimensional chaos in impulsed linear oscillating circuits," *Int. J. Bifurcation and Chaos* **3**(4), 921–941.

Gardini, L., Mira, C. & Fournier-Prunaret, D. [1992] "Properties of invariant areas in two-dimensional endomorphisms," *Proceedings of the European Conference on Iteration Theory* (Batschuns, Austria, Sept. 1992), in press.

Grebogi, C., Ott, E. & Yorke, J. A. [1983] "Fractal basin boundaries, long-lived chaotic transients, and unstable-unstable pair bifurcations," *Phys. Rev. Lett.* **50**, 935–938.

Gumowski, I. & Mira, C. [1975a] "Sur les récurrences, ou transformations ponctuelles, du premier ordre, avec inverse non-unique," *C.R. Acad. Sci. Paris*, t. 280, Série A, 905–908.

Gumowski, I. & Mira, C. [1975b] "Structure de bifurcations boites-emboitées dans les récurrences du premier ordre dont la fonction présente un seul extrémum," *C.R. Acad. Sci. Paris*, t. 282, Série A, 219–222.

Gumowski, I. & Mira, C. [1975c] "Accumulations de biforcations dans une récurrence," *C.R. Acad. Sci. Paris*, t. 281, Série A, 45–48.

Gumowski, I. & Mira, C. [1977] "Solutions chaotiques bornées d'une récurrence ou transformation ponctuelle du deuxiéme ordre, à inverse non unique," *C.R. Acad. Sci. Paris*, t. 285, Série A, 447–470.

Gumowski, I. & Mira, C. [1978] "Bifurcation destabilisant une solution chaotique d'un endomorphisme de 2e ordre," *C.R. Acad. Sci. Paris*, t. 286, Série A, 427–431.

Gumowski, I. & Mira, C. [1980a] *Dynamique Chaotique* (Cepadues Editions, Toulouse).

Gumowski, I. & Mira, C. [1980b] *Recurrences and Discrete Dynamical Systems* (Springer-Verlag, New York).

Hogg, T. & Huberman, B. A. [1984] "Generic behavior of coupled oscillators," *Phys. Rev.* **A29**, 275–281.

Kaneko, K. [1983] "Collapse of tori and genesis of chaos in non-linear nonequilibrium systems," Dr. Thesis, Dep. of Physics, University of Tokyo.

Li, T.-Y. & Yorke, J. A. [1975] "Period three implies chaos," *Amer. Math. Monthly* **82**, 985–992.

López-Ruiz, R. & Pérez-Garcia, C. [1992] "Dynamics of two logistic maps with a multiplicative coupling," *Int. J. Bifurcation and Chaos* **2**(2), 421–425.

Lorenz, E. N. [1989] "Computational chaos — A prelude to computational instability," *Physica* **D35**, 299–317.

Marotto, J. R. [1978] "Snap-back repellers imply chaos in R^n," *J. Math. Analysis Appl.* **63**, 199–223.

Mira, C. [1965] "Détermination pratique du domaine de stabilité d'un point d'équilibre d'une récurrence non-lineaire du deuxiéme ordre à variables réelles," *C.R. Acad. Sci. Paris*, t. 261, 5314–5317, Groupe 2.

Mira, C. [1966] "Sur quelques propriétés de la frontiére de stabilité d'un point double d'une récurrence et sur un cas de biforcation de cette frontiére," *C.R. Acad. Sci. Paris*, t. 262, Série A, 951–954.

Mira, C. & Roubellat, F. [1969] "Cas ou le domaine de stabilité d'un ensemble limite attractif d'une récurrence du deuxiéme ordre n'est pas simplement connexe," *C.R. Acad. Sci. Paris*, t. 268, Série A, 1675–1678.

Mira, C. [1975] "Accumulations de biforcations et structures boites-emboitées dans les récurrences et transformations ponctuelles," in *Proceedings of the VII International Conference on Non-Linear Oscillations, Berlin, Sept. 1975* (Akademic Verlag, Berlin, 1977) pp. 81–93.

Mira, C. [1980] "Complex dynamics in two-dimensional endomorphisms," *Nonlinear Analysis, T.M. & A.* **4**, 1167–1187.

Mira, C. [1987] *Chaotic Dynamics* (World Scientific, Singapore).

Mira, C. [1992] Private communication.

Mira, C. & Narayaninsamy, T. [1993] "On two behaviors of two-dimensional endomorphisms. Role of the critical curves," *Int. J. Bifurcation and Chaos* **3**(1), 187–194.

Taylor, J. G. [1990] "Noisy neural net states and their time evolution," *SIAM J. Appl. Math.* **50**, 1073–1087.

Van Biskirk, R. & Jeffries, C. [1985] "Observation of chaotic dynamics of coupled nonlinear oscillators," *Phys. Rev.* **A31**, 3332–3357.